Tanjona R. Rabemananjara
In Collab. W/ A. Candido, A. Garcia, G. Magni, J. Rojo, R. Stegeman
27th CAN Symposium on Astroparticle Physics - June 21, 2023
Soesterberg, Netherlands

Based on arXiv:2302.08527 / 10.1007/JHEP05(2023)149

Introduction & Motivations

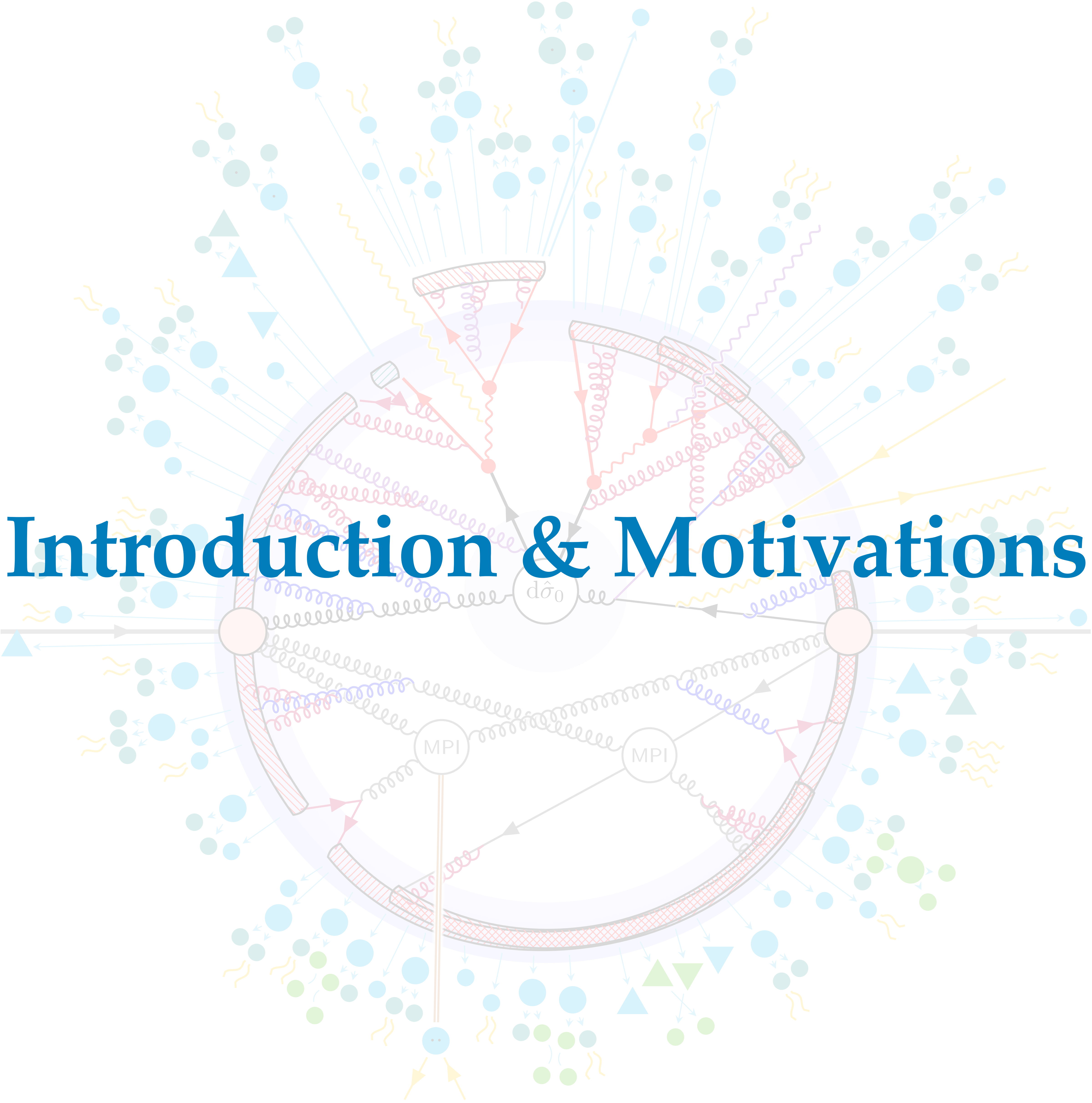

Introduction & Motivations

Interpretation of present and future neutrino **experiments** requires **accurate theoretical predictions for neutrino-nucleon/nucleus scattering rates**

Introduction & Motivations

Inclusive neutrino cross-section receives **sizeable contributions** from $Q < 2$ GeV where QCD calculations cannot be evaluated in the pQCD framework

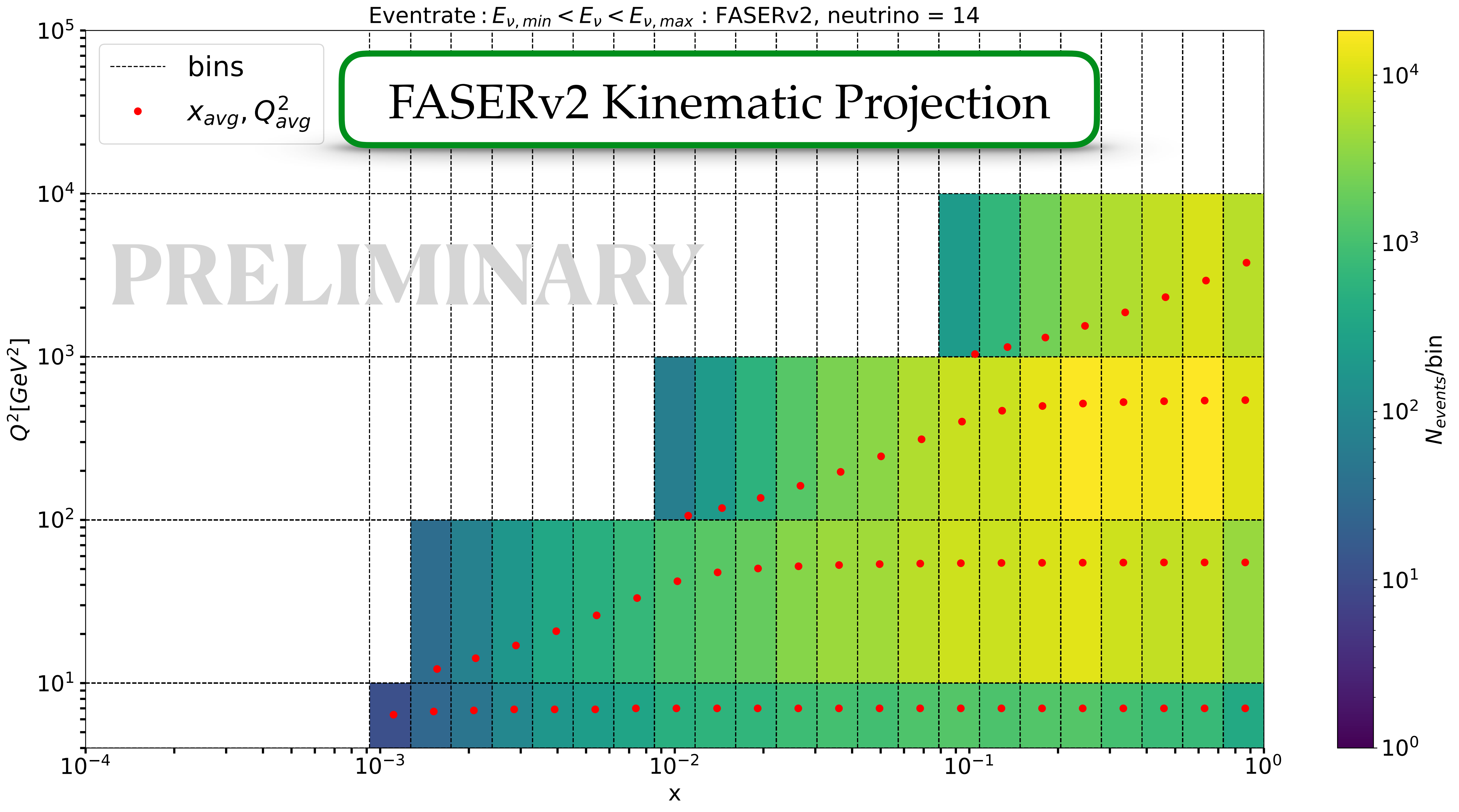

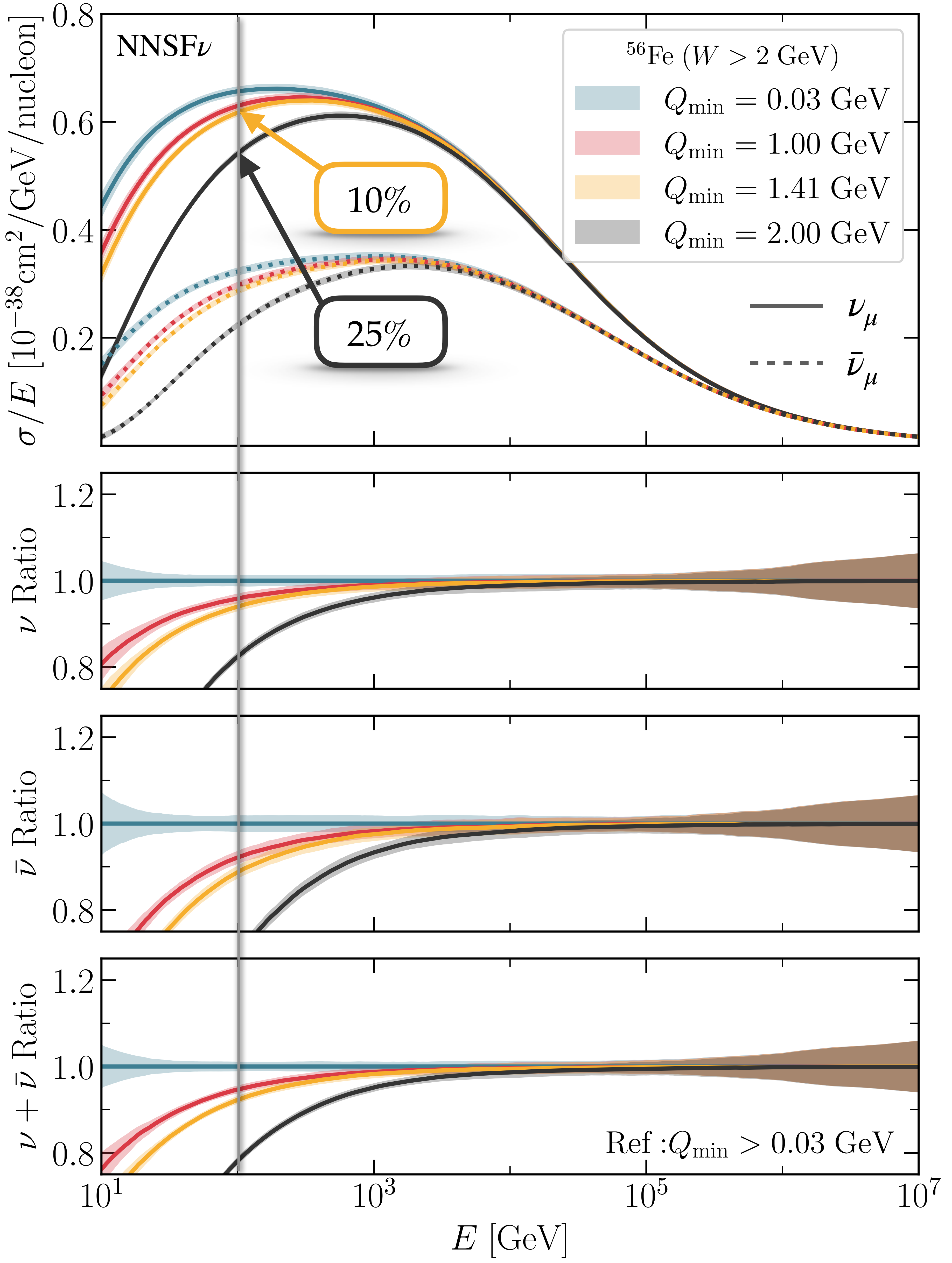

In Collaboration with M. Fieg, T. Giani, P. Krack, T. Rabemananjara, T. Mäkelä, J. C. Martinez, J. Rojo

Relevance of low-Q^2 Regions

In **muon-neutrino inelastic scattering**, at $E_\nu \sim$ few GeV, the total cross-section is determined entirely by the **low-Q^2 regions:**

$$\sigma(E_\nu) = \int_{Q^2_{\min}}^{2m_N E_\nu} dQ^2 \int_{Q^2/(2m_N y E_\nu)}^{1} dx \left[\frac{d^2\sigma}{dx dQ^2}(x, Q^2, E_\nu) \equiv \sum_i \mathscr{C}_i F_i(x, Q^2) \right]$$

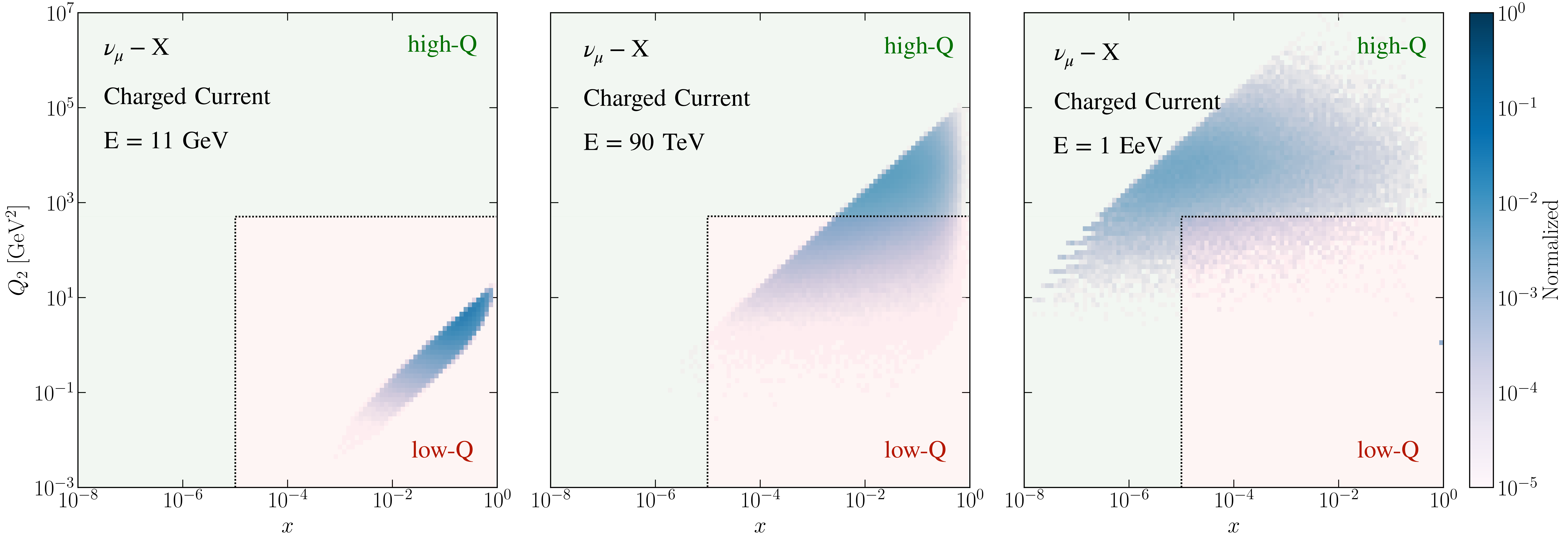

Model the low-Q^2: Bodek-Yang (BY)

BY is based on **Effective LO Parton Distribution Functions (PDFs)** (GRV98LO) with modified scaling variables and K-factors to approximate higher-order QCD corrections:

$$f_i^{\rm LO}(x, Q^2) \longrightarrow f_i^{\rm LO}(\xi, Q^2), \quad \text{with} \quad \xi = \frac{2x(Q^2 + m_f^2 + B)}{2Ax + \left[1 + \sqrt{1 + (2m_N x)^2/Q^2}\right]}$$

Shortcomings of the BY model:

- **Obsolete PDF parametrisation** that neglects constraints on proton & nuclear structure in the last 25 years
- **Neglect higher-order perturbative QCD calculations** (which can be significant)
- **Cannot be matched** to calculations of **high-energy neutrino scattering** based on modern PDF and higher-QCD calculations, introducing an unnecessary **separation between modelling of neutrino interactions** sensitive to **different energy regions**.
- **Lack** of **systematic estimate of the uncertainties** associated to the predictions $\iff \nexists$ **degree of belief**

NNSFν: Using state-of-the-art ML and QCD computations

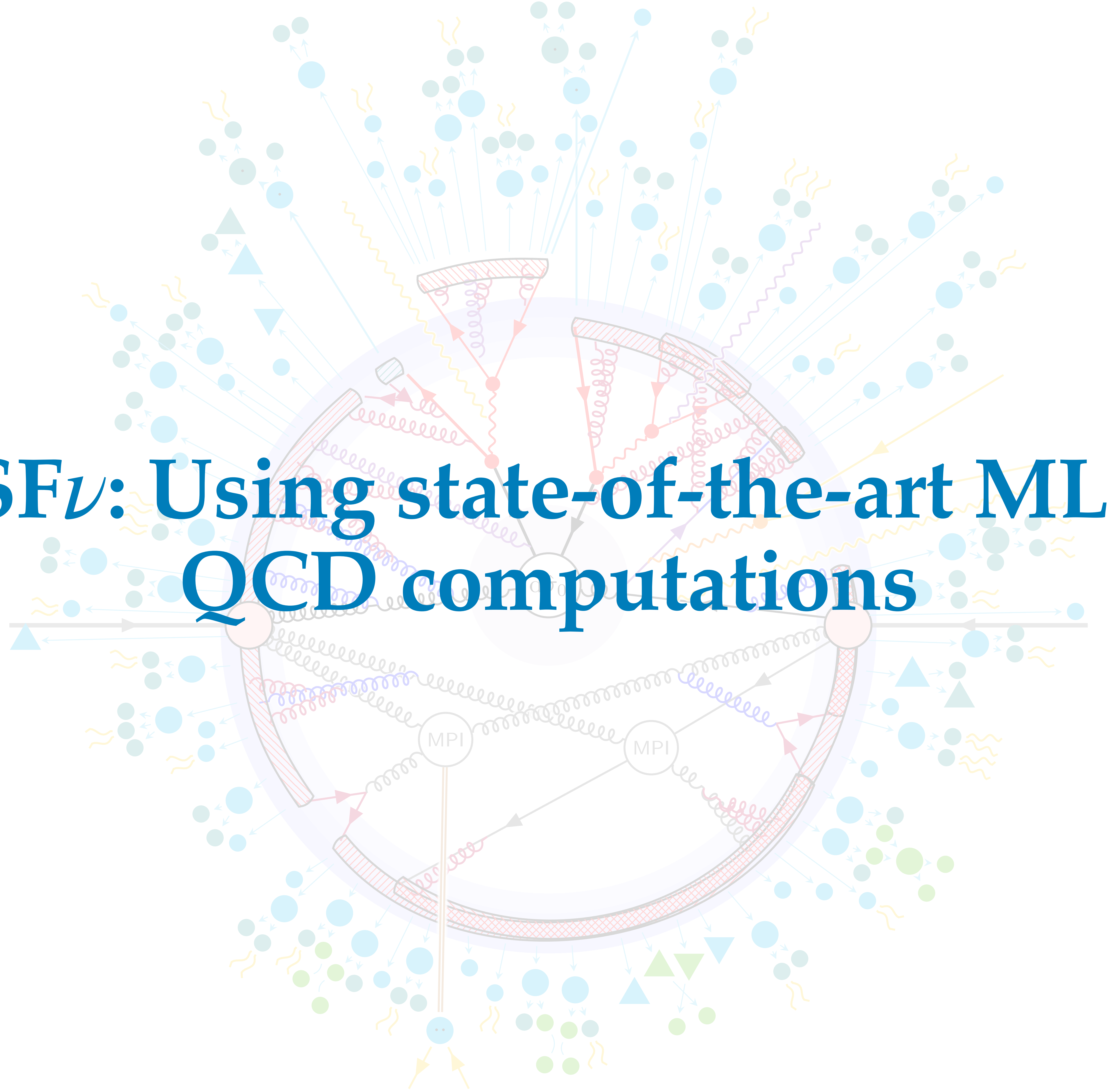

NNSFν: The Approach

- Use available **data** on neutrino-nucleus scattering to **parametrise and determine the inelastic structure functions** using a NN as an unbiased interpolant
- The parametrisation is done in such a way that it **converges to the pQCD calculations at large enough Q^2**
- In the region where neutrino energy is sensitive to **large-Q^2**, the parametrisation is **replaced by pQCD calculations**

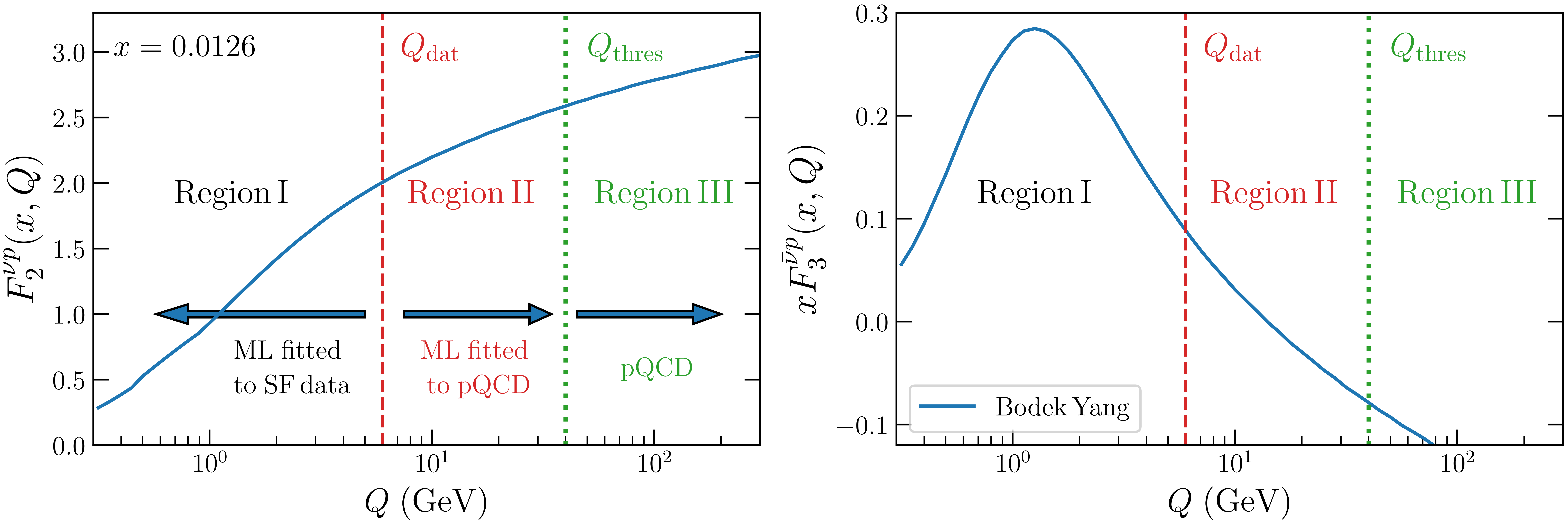

NNSFν: Experimental Inputs

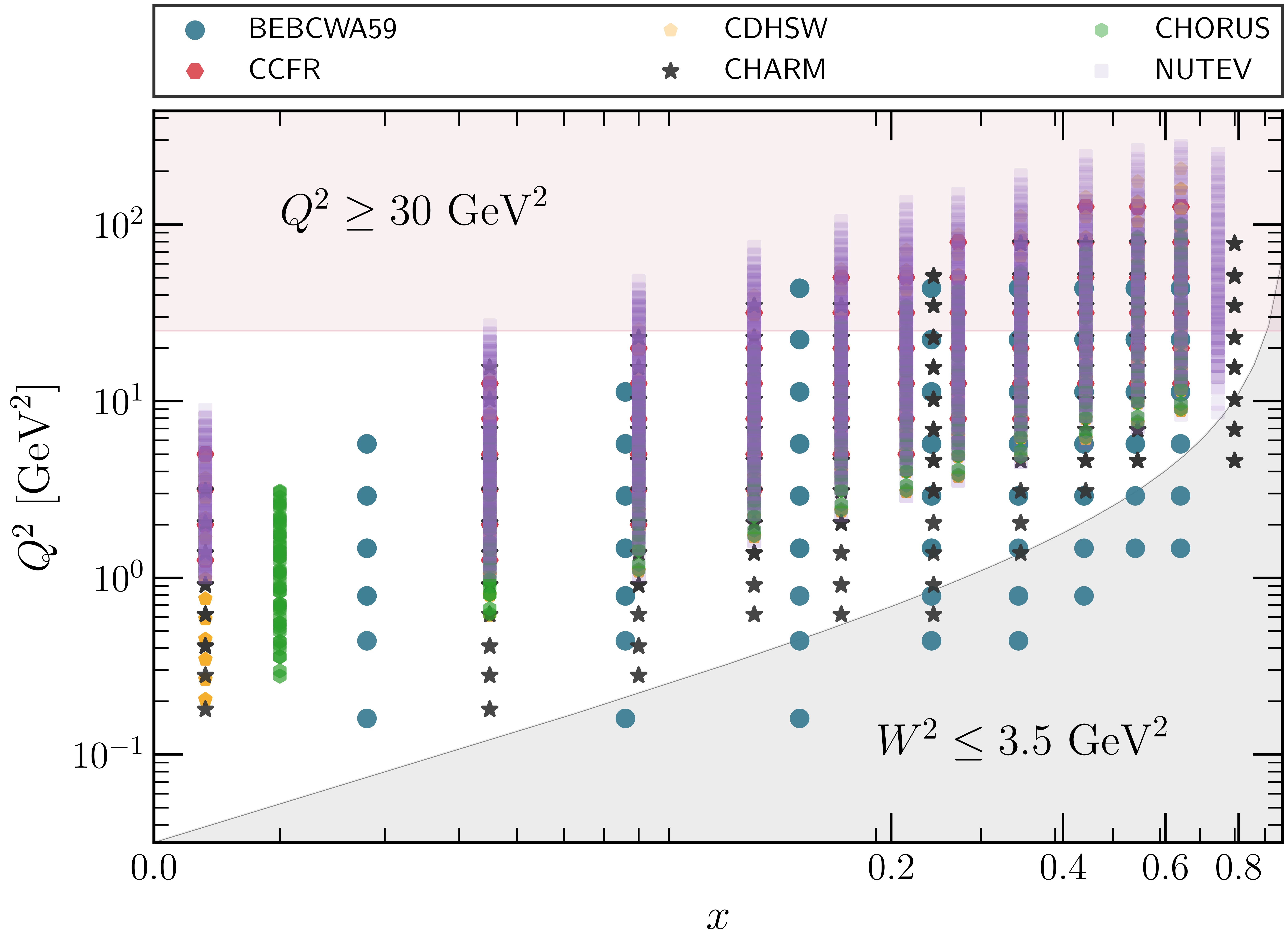

- The datasets include various **observables**, **scattering target**, and **final state** that amounts to 6224 (4184) before (after) the cut.
- The datasets span a **wide range of kinematics**. Two different types of **cuts** are applied to the experimental datasets: W^2 and Q^2_{max}.
- The resulting **determination** of neutrino inelastic structure functions are **valid for ~12 orders of magnitude in E_ν**, from ~few GeV to 10^{12} GeV.

NNSFν: Methodology

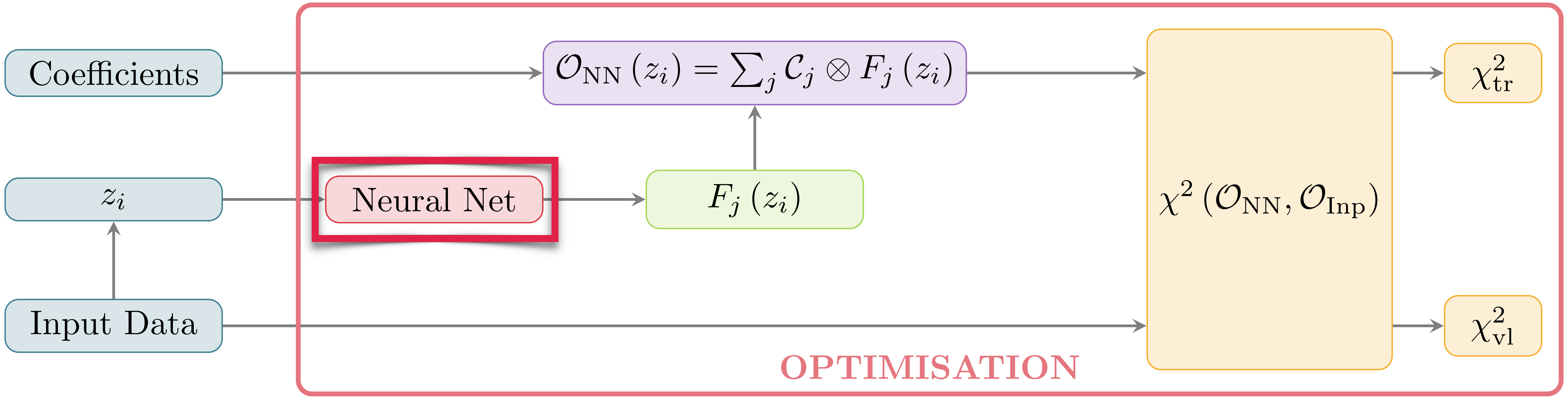

Training/Optimisation: observable definition, stopping criteria, etc.

NNSFν: Methodology

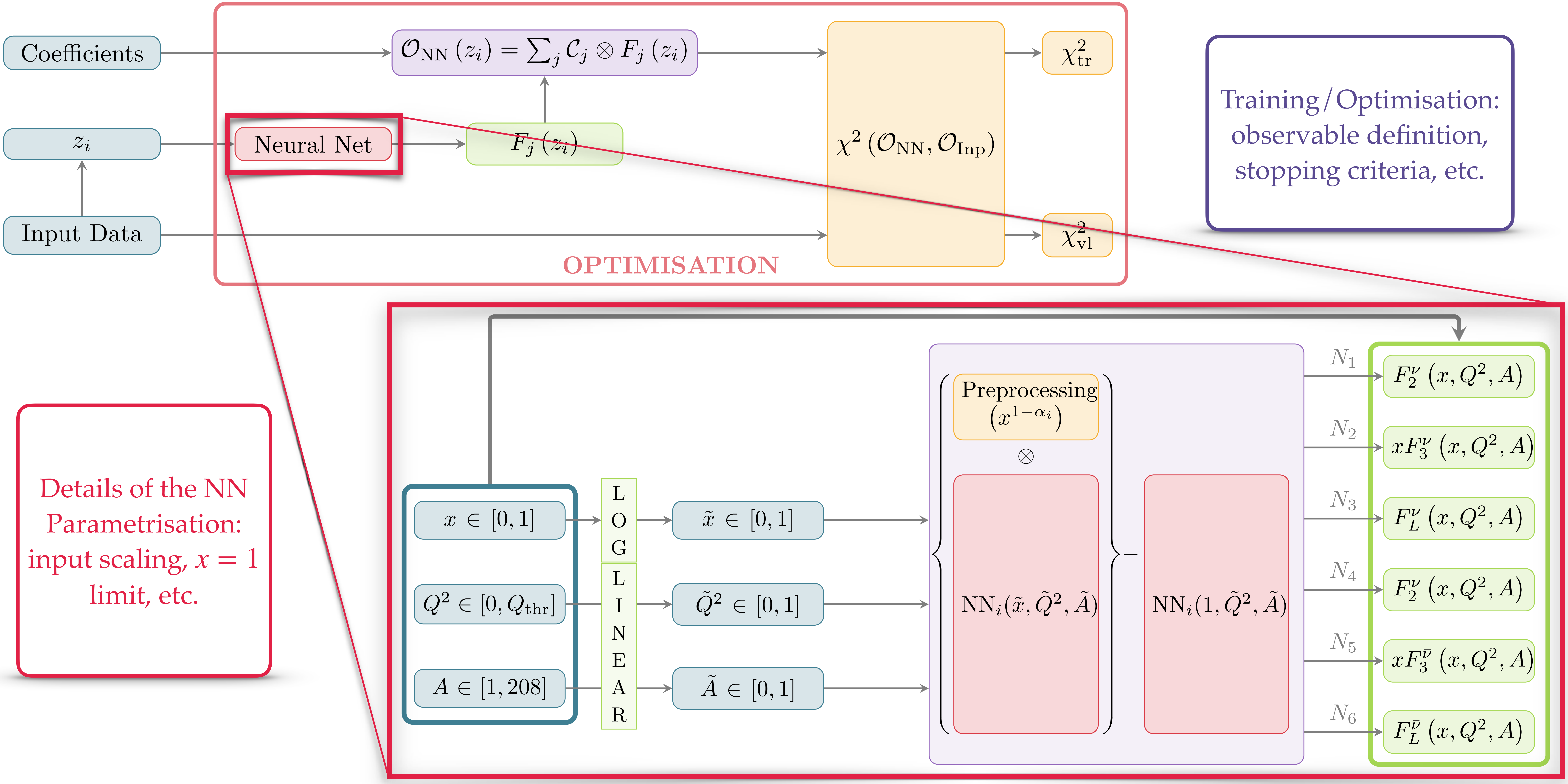

Training/Optimisation: observable definition, stopping criteria, etc.

Details of the NN Parametrisation: input scaling, $x = 1$ limit, etc.

NNSFν: Neutrino Structure Function Predictions

Smooth transition between data-driven & pQCD computations with proper uncertainty estimate in whole Q range

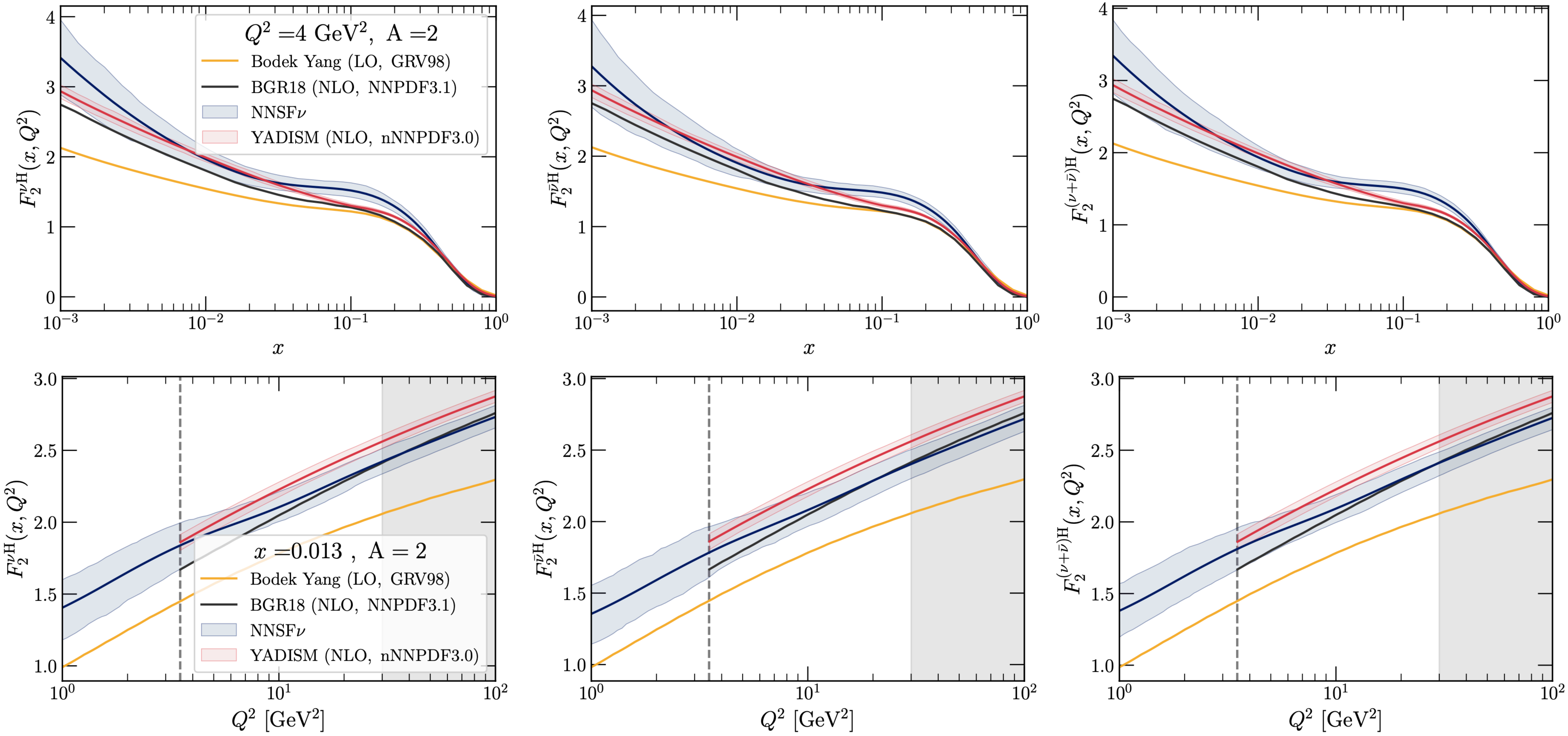

NNSFν: Interpolation along A

The advantage of parametrising A is that one can generate predictions for nuclei for which direct experimental measurements are not available. To illustrate this we compare two fits in which $A = 20$ is removed in one.

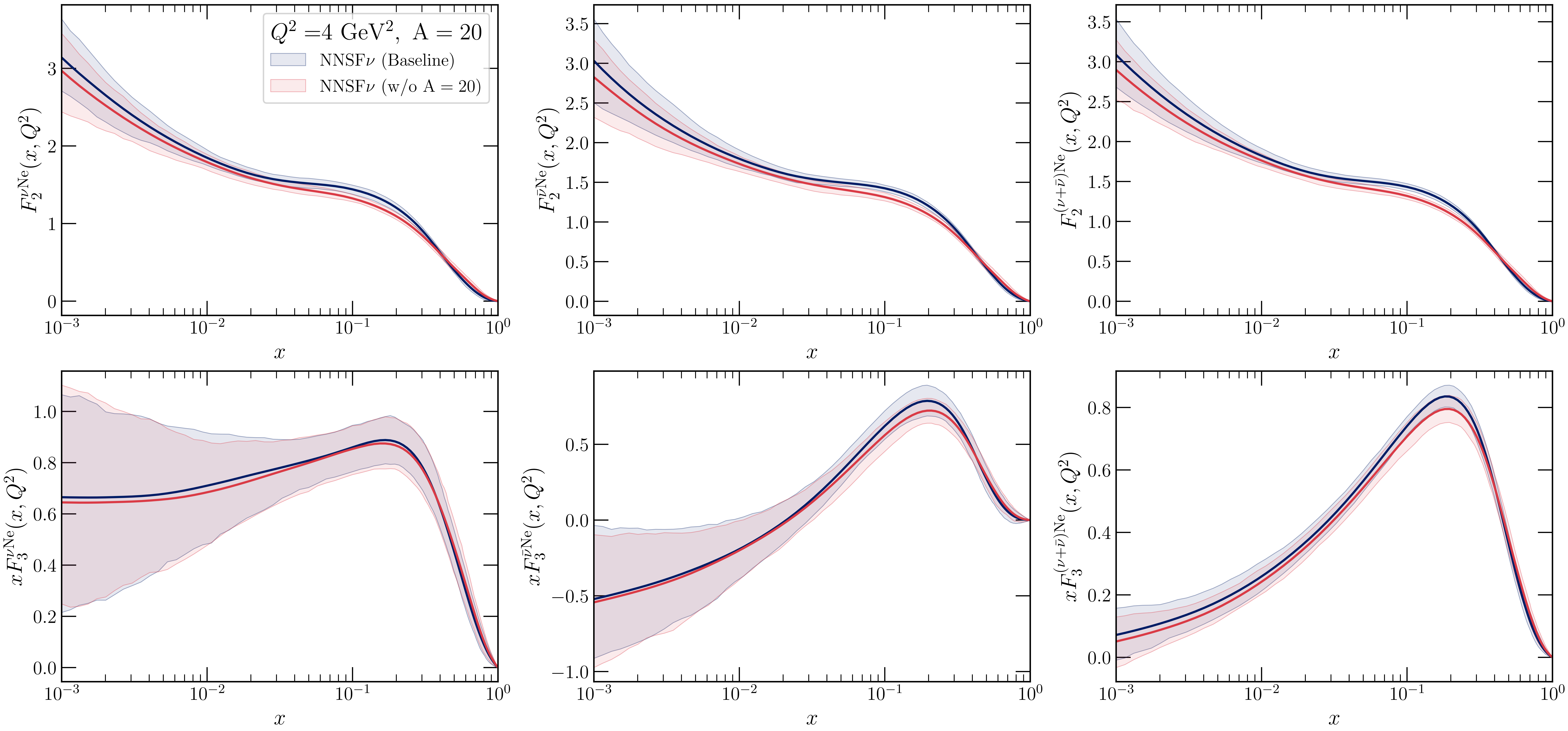

Phenomenology of Inclusive Neutrino Cross-Sections

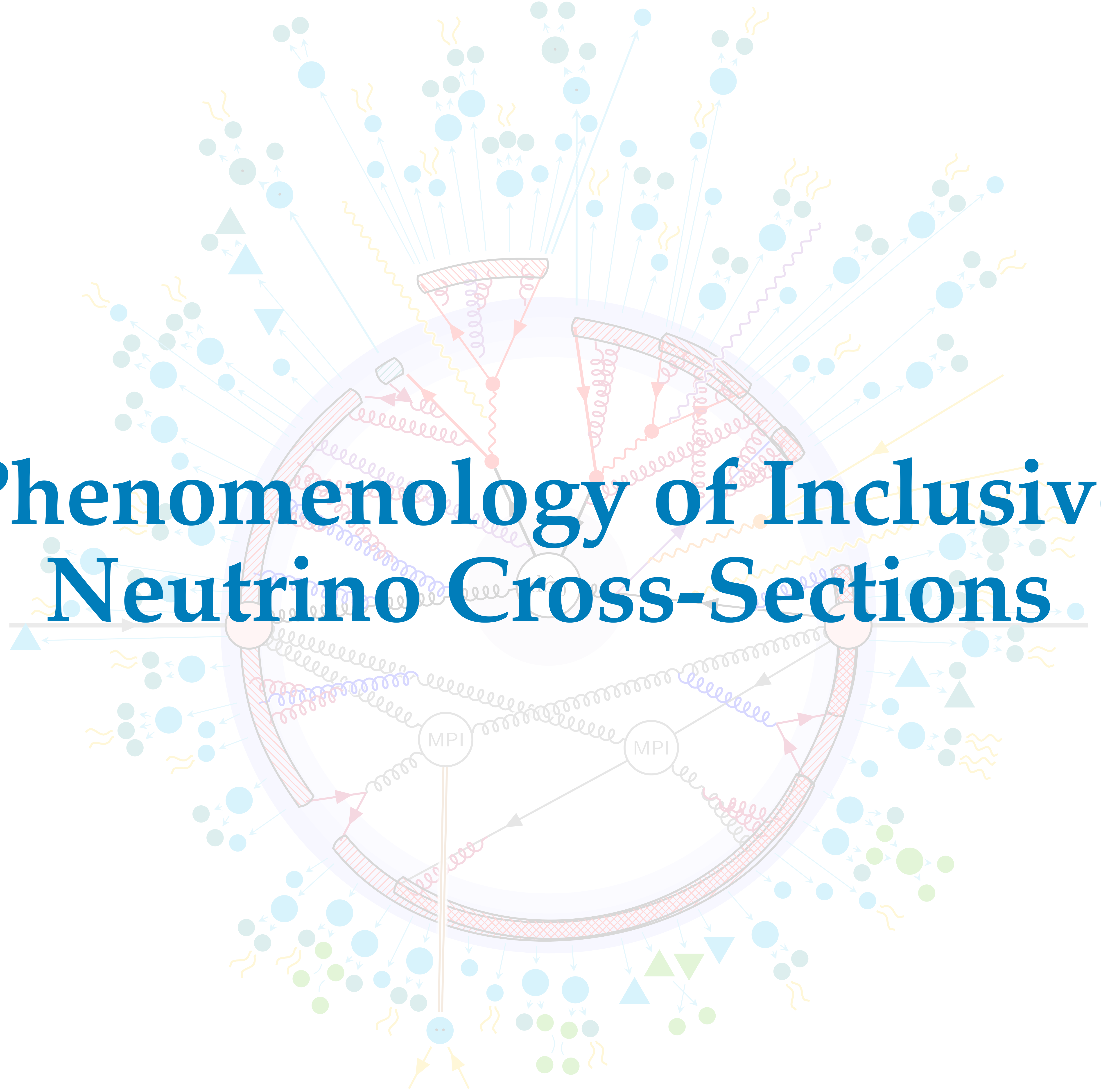

NNSFν: Inclusive Neutrino-Nucleus Cross-Sections

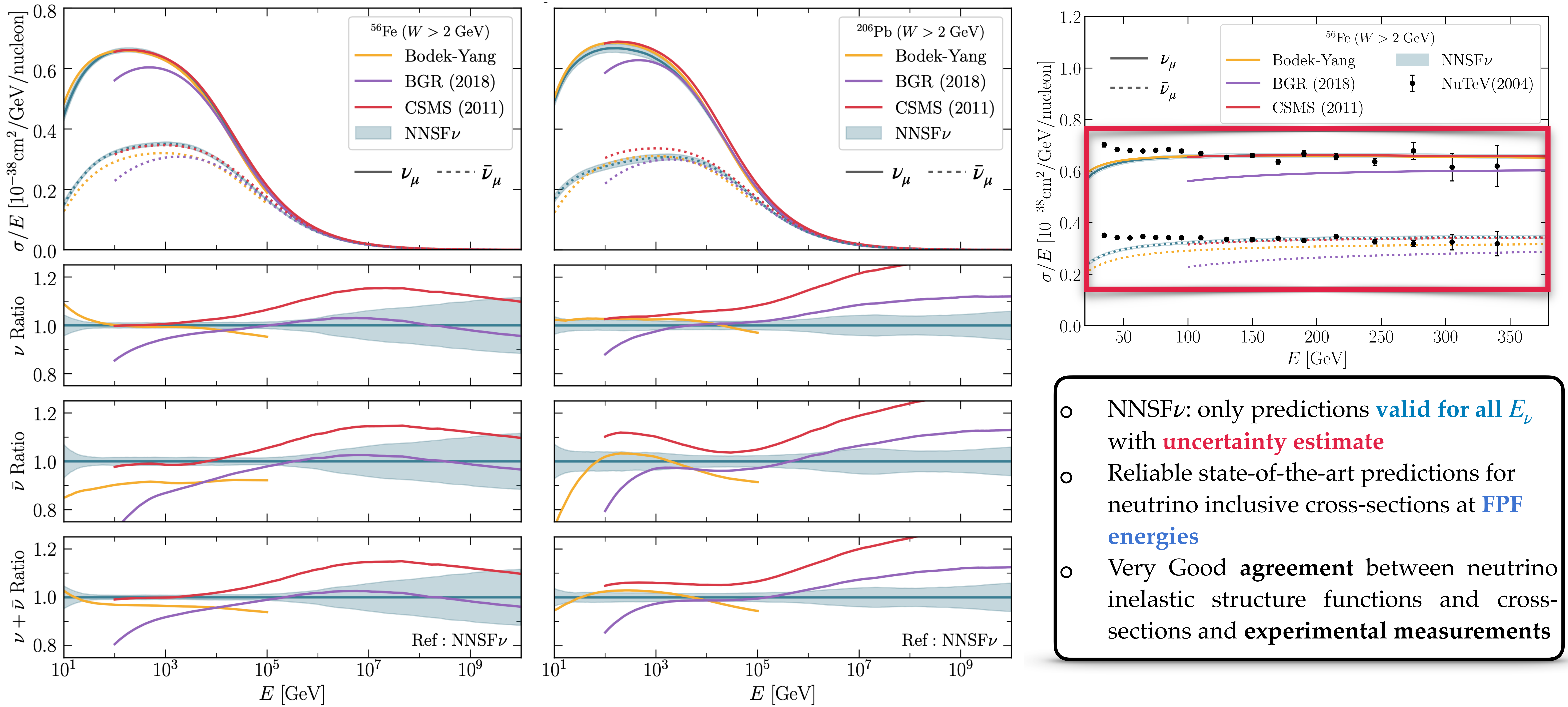

- NNSFν: only predictions **valid for all E_ν** with **uncertainty estimate**
- Reliable state-of-the-art predictions for neutrino inclusive cross-sections at **FPF energies**
- Very Good **agreement** between neutrino inelastic structure functions and cross-sections and **experimental measurements**

NNSFν: Inclusive Neutrino-Nucleus Cross-Sections

Delivery & Usage

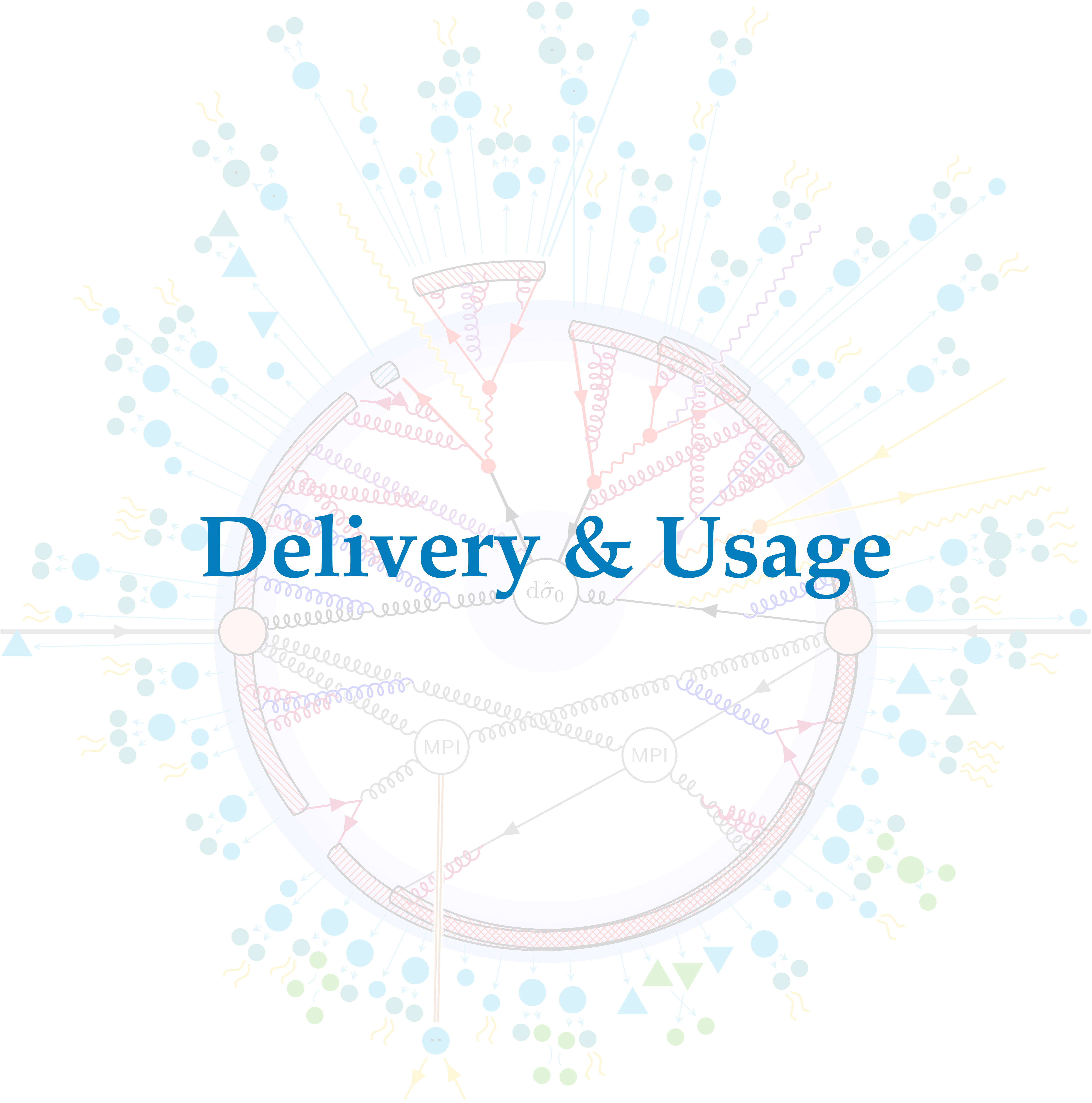

Adopting FOSS Philosophy

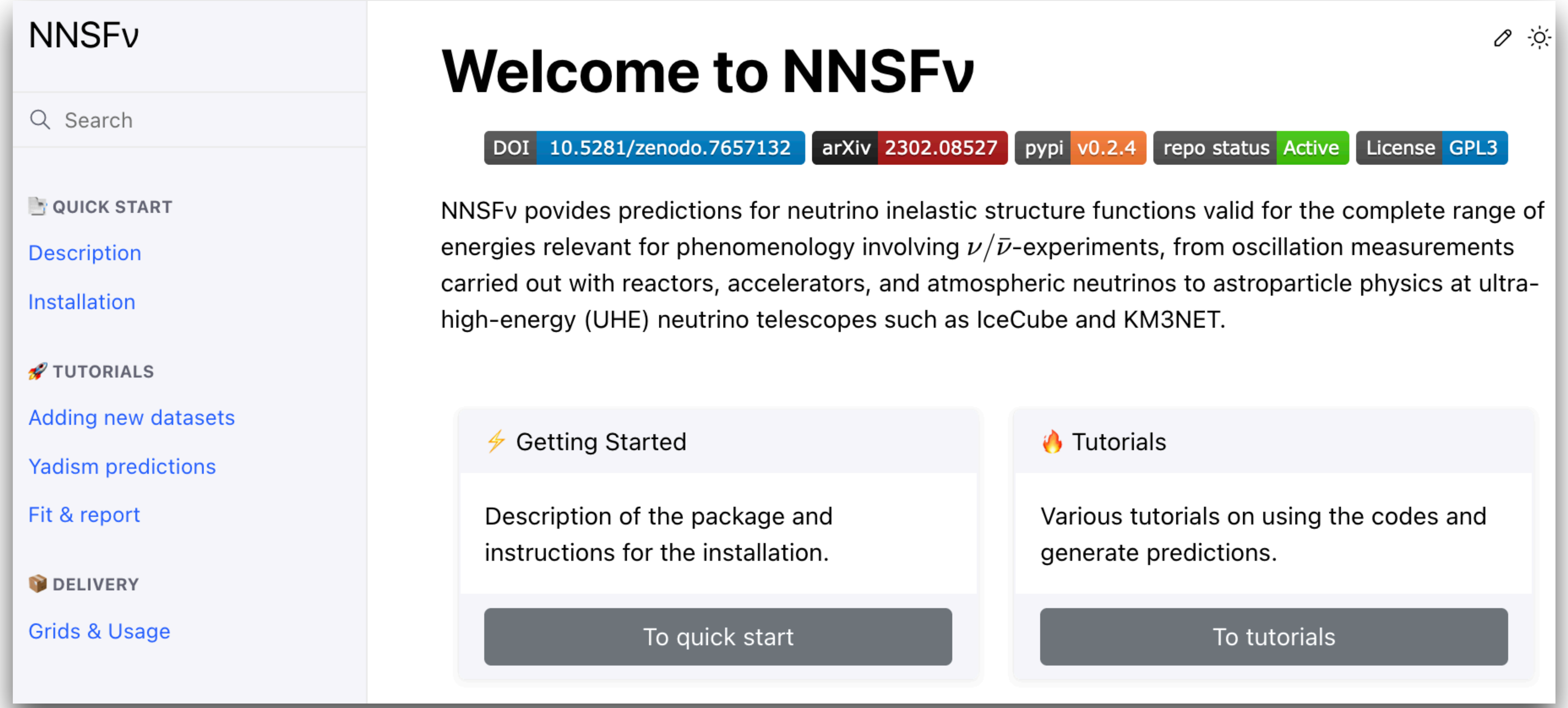

The code is publicly available at the following link:
https://github.com/NNPDF/nnusf
Documentation along with tutorials are available at:
https://nnpdf.github.io/nnusf/

NNSFν is interfaced with the GENIE MC Generator:
http://genie-mc.org/

NNSFν grids are tabulated in the LHAPDF format:
https://lhapdf.hepforge.org/index.html

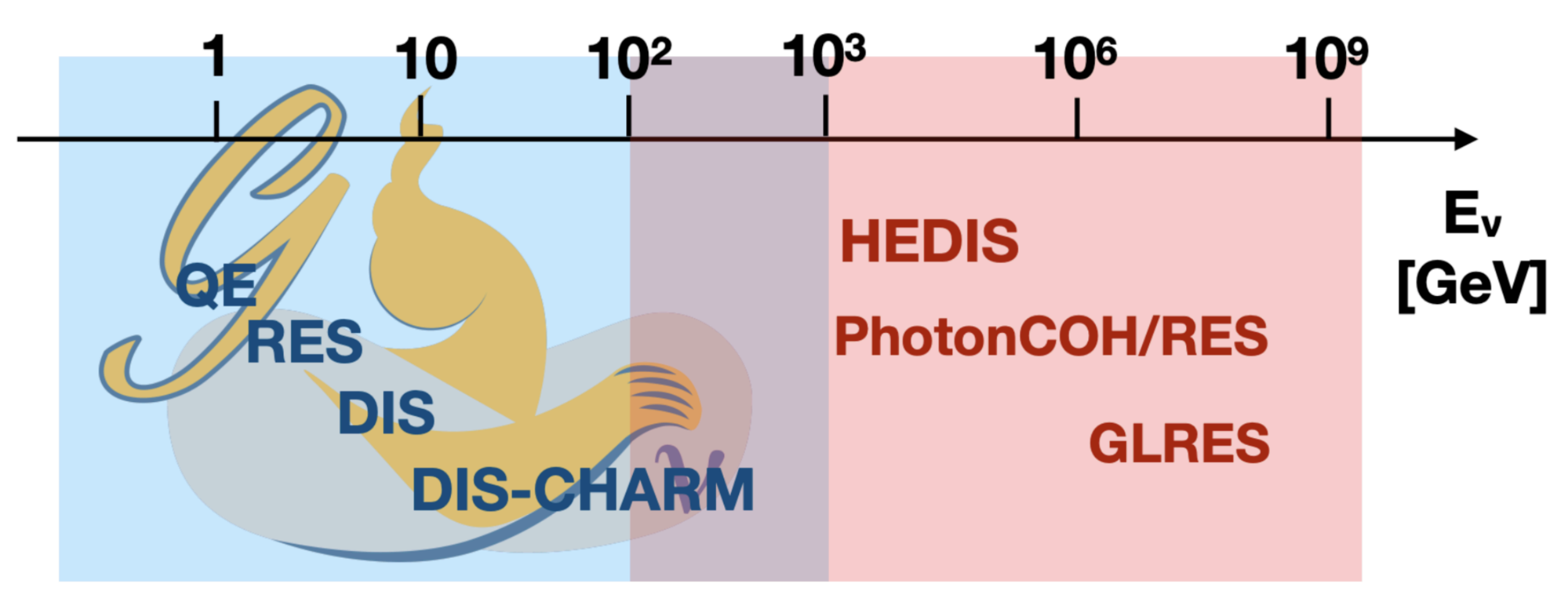

UNIVERSAL NEUTRINO GENERATOR & GLOBAL FIT

(Z, A) [target]	Low-Q Grid	High-Q Grid
$(1, 2)$	NNSFnu_D_lowQ	NNSFnu_D_highQ
$(2, 4)$	NNSFnu_He_lowQ	NNSFnu_He_highQ
$(3, 6)$	NNSFnu_Li_lowQ	NNSFnu_Li_highQ
$(4, 9)$	NNSFnu_Be_lowQ	NNSFnu_Be_highQ
$(6, 12)$	NNSFnu_C_lowQ	NNSFnu_C_highQ
$(7, 14)$	NNSFnu_N_lowQ	NNSFnu_N_highQ
$(8, 16)$	NNSFnu_O_lowQ	NNSFnu_O_highQ
$(13, 27)$	NNSFnu_Al_lowQ	NNSFnu_Al_highQ
$(15, 31)$	NNSFnu_Ea_lowQ	NNSFnu_Ea_highQ
$(20, 40)$	NNSFnu_Ca_lowQ	NNSFnu_Ca_highQ
$(26, 56)$	NNSFnu_Fe_lowQ	NNSFnu_Fe_highQ
$(29, 64)$	NNSFnu_Cu_lowQ	NNSFnu_Cu_highQ
$(47, 108)$	NNSFnu_Ag_lowQ	NNSFnu_Ag_highQ
$(50, 119)$	NNSFnu_Sn_lowQ	NNSFnu_Sn_highQ
$(54, 131)$	NNSFnu_Xe_lowQ	NNSFnu_Xe_highQ
$(74, 184)$	NNSFnu_W_lowQ	NNSFnu_W_highQ
$(79, 197)$	NNSFnu_Au_lowQ	NNSFnu_Au_highQ
$(82, 208)$	NNSFnu_Pb_lowQ	NNSFnu_Pb_highQ

Conclusions & Outlook

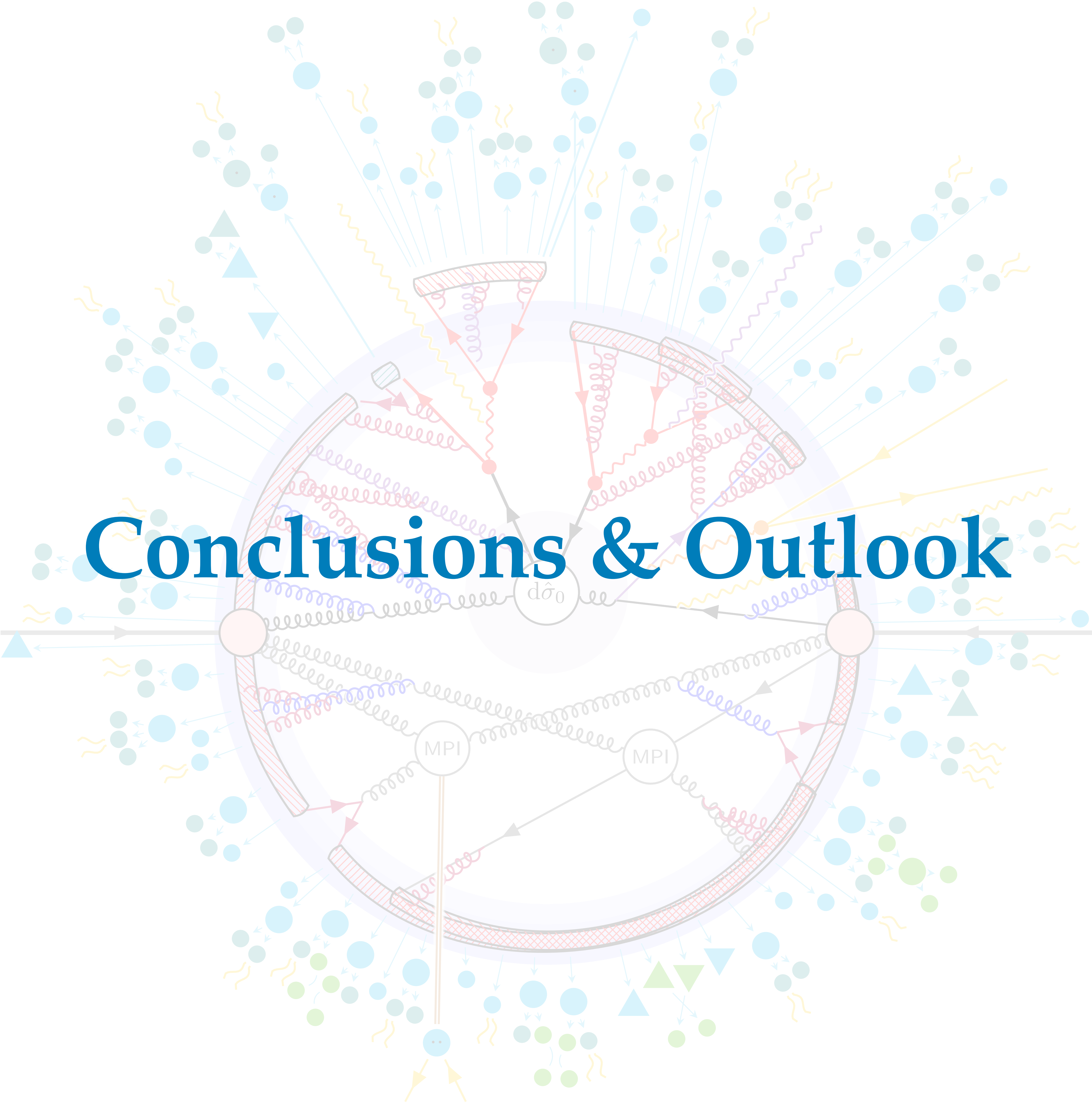

Summary

- Accurate predictions for scattering rate of neutrino-nucleus interactions play a crucial role in interpretation of present neutrino experiments
- The **low-Q^2 regions contribute to a significant degree to the inclusive neutrino inelastic cross-sections**
- State-of-the-art methods relying on Machine Learning provide an unbiased and better predictions for low-energy neutrino physics
- NNSFν predictions for inelastic neutrino structure functions and cross-sections are valid for all energies relevant for neutrino phenomenology and are **available as interpolation grids in the LHAPDF format & as an interface with GENIE**
- Precision QCD and neutrino physics at future experiments will benefit from precision neutrino structure functions

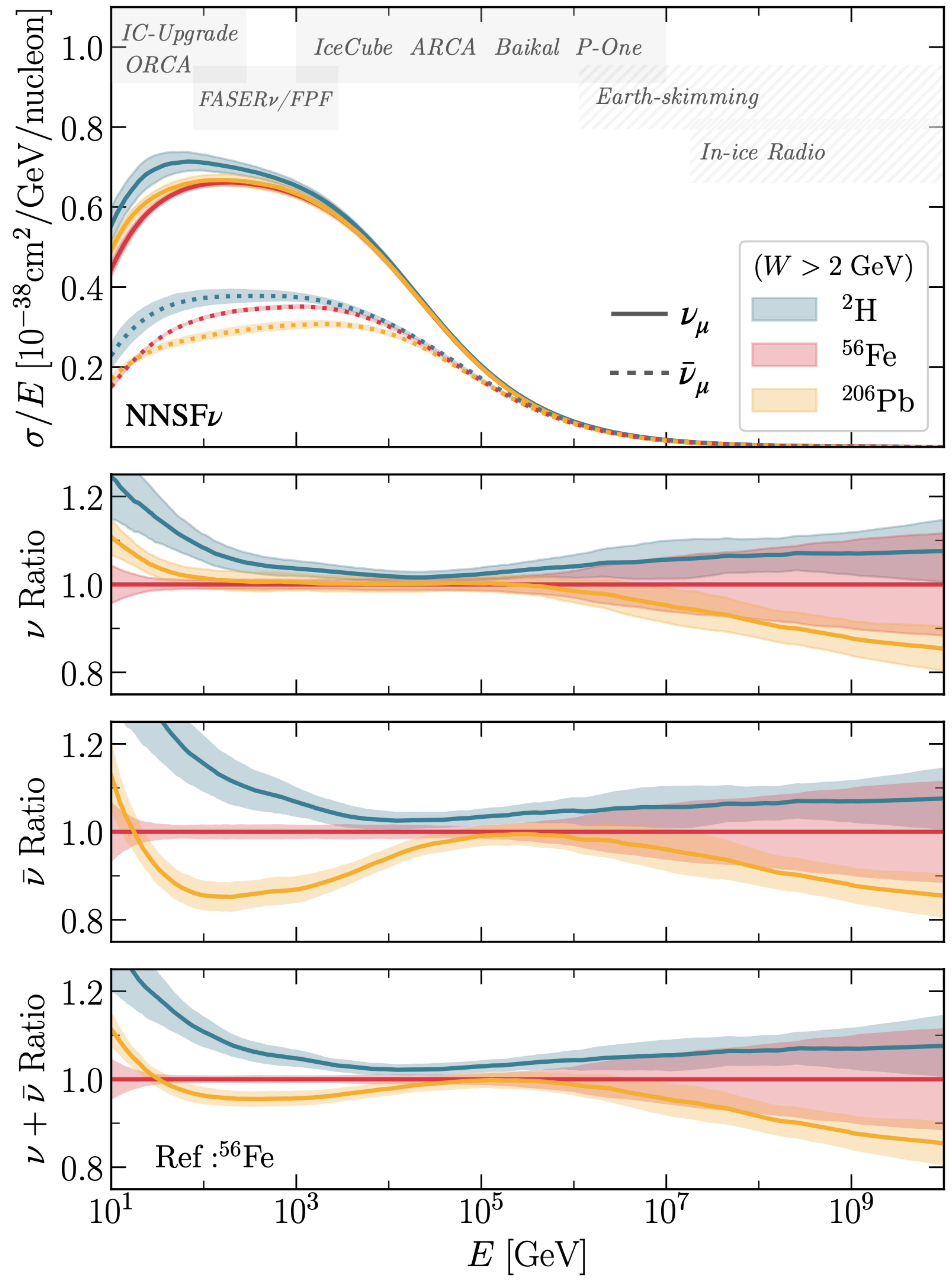

Backup Slides

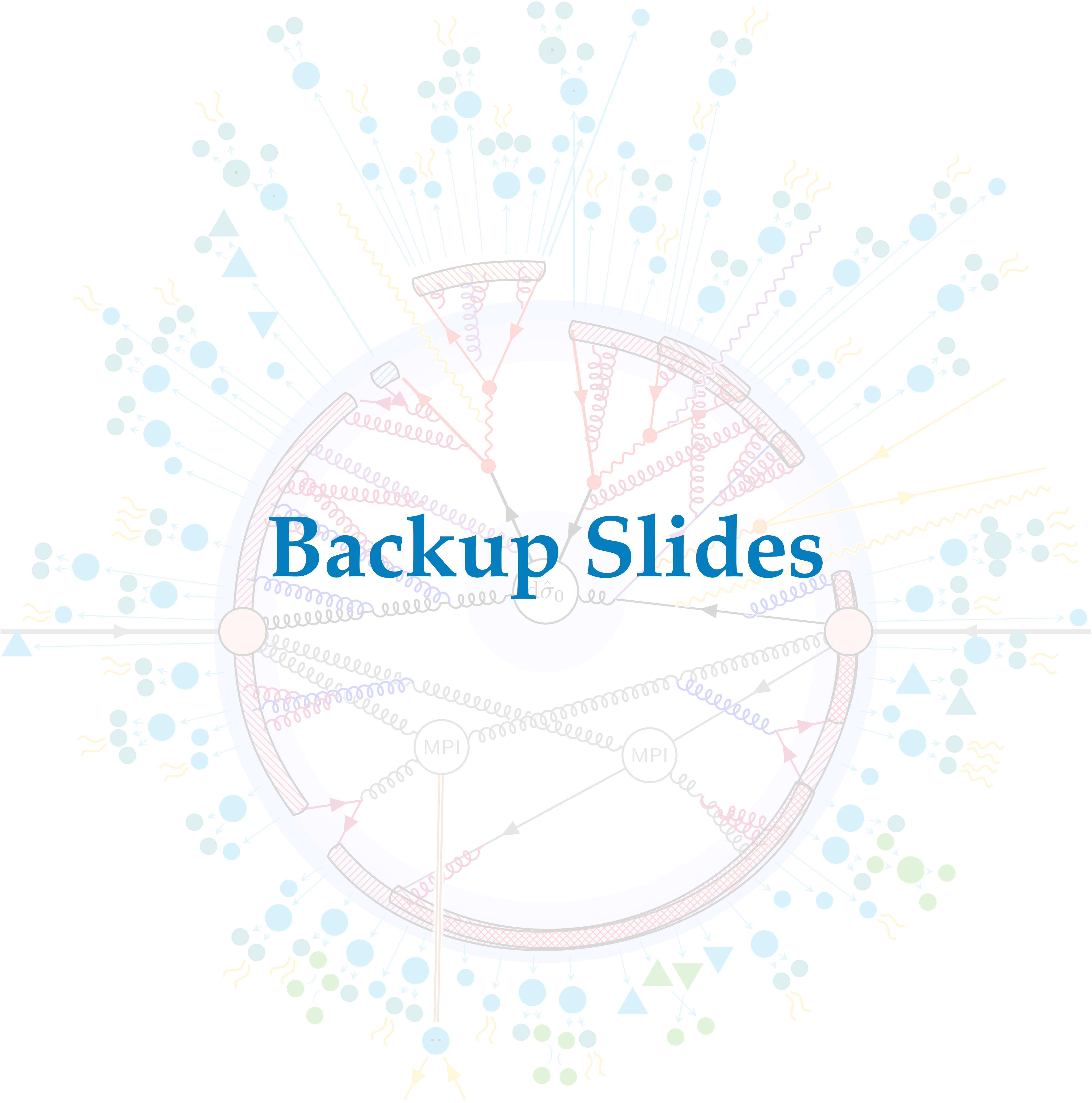

Model the low-Q^2: Bodek-Yang

Bodek-Yang (BY) is based on Effective **LO PDFs** (GRV98LO) with **modified scaling variables** and **K-factors** to approximate higher-order QCD corrections:

$$f_i^{\mathrm{LO}}(x, Q^2) \longrightarrow f_i^{\mathrm{LO}}(\xi, Q^2), \quad \text{with} \quad \xi = \frac{2x(Q^2 + m_f^2 + B)}{2Ax + \left[1 + \sqrt{1 + (2m_N x)^2/Q^2}\right]}$$

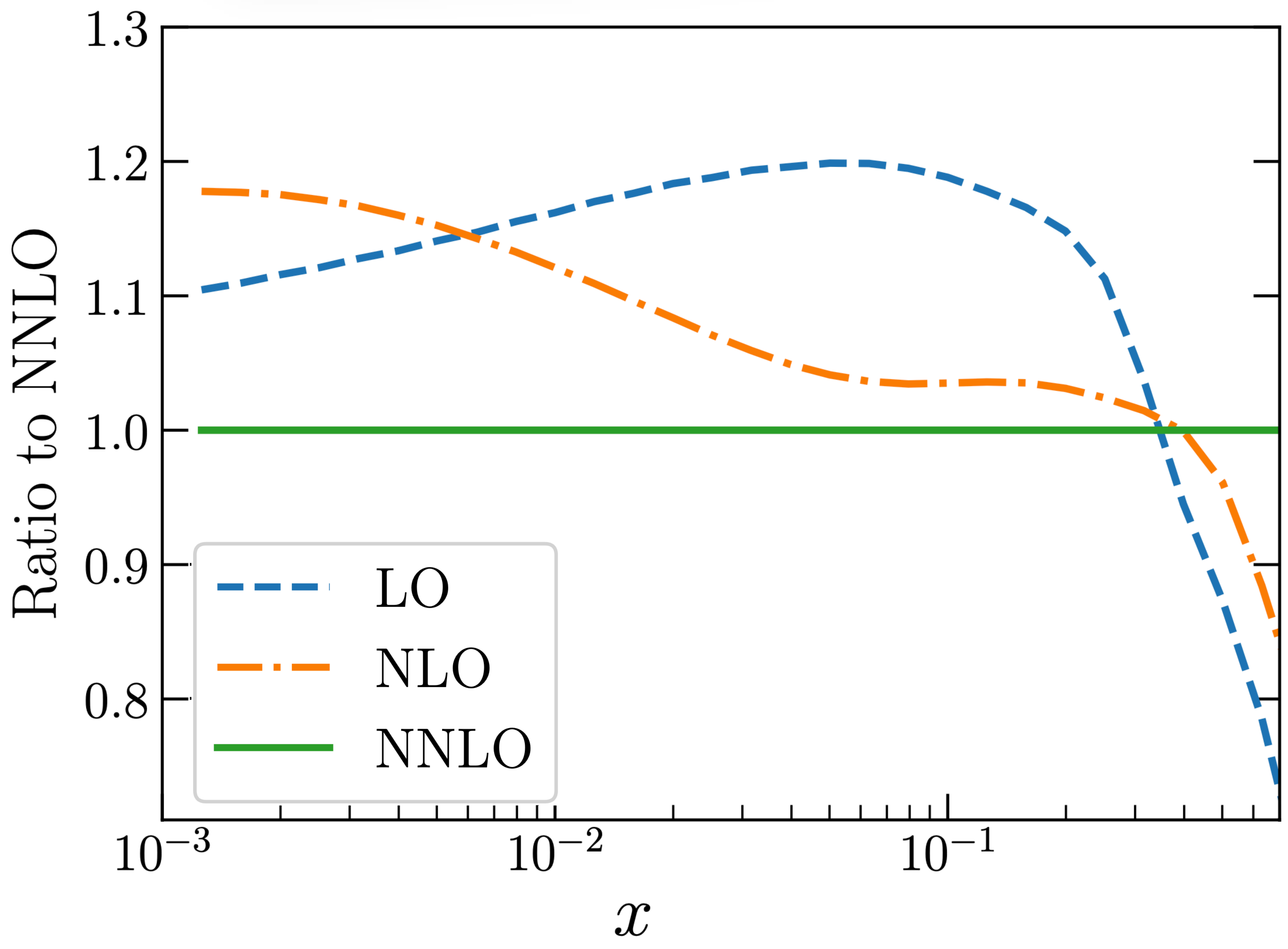

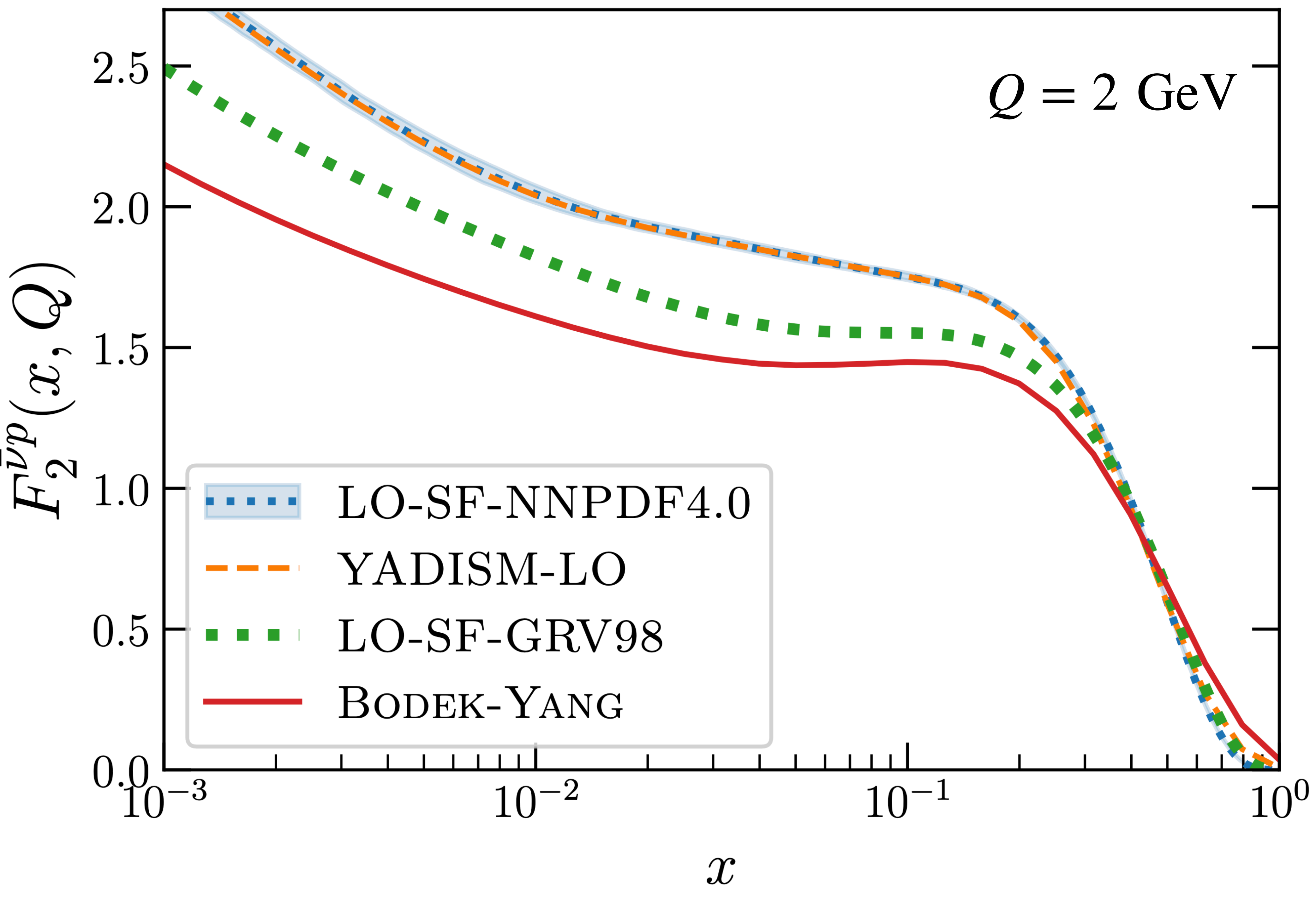

- **LO** predictions can be up to **25%** higher wrt NNLO
- **NLO** predictions can be up to **20%** higher wrt NNLO
- **BY** predictions depart from best QCD predictions even at moderate Q

Status of the Yadism Code

NLO	light	heavy	intrinsic	asymptotic
NC	✓	✓	✓	✓
CC	✓	✓	✓	✓
NNLO				
NC	✓	✓	✗	✓
CC	✓	tabulated*	✗	✓
N3LO				
NC	✓	✗†	✗	✗‡
CC	✓	✗†	✗	✗

* Already available as K-factors [64], now being integrated in the grid format.

† Full calculation not available but an approximated expression can be constructed from partial results [105, 106].

‡ Calculation available, to be implemented.

Overview of the different types and accuracy of the DIS coefficient functions currently implemented in YADISM

https://yadism.readthedocs.io/en/latest/

Contributions from the Individual Structure Functions

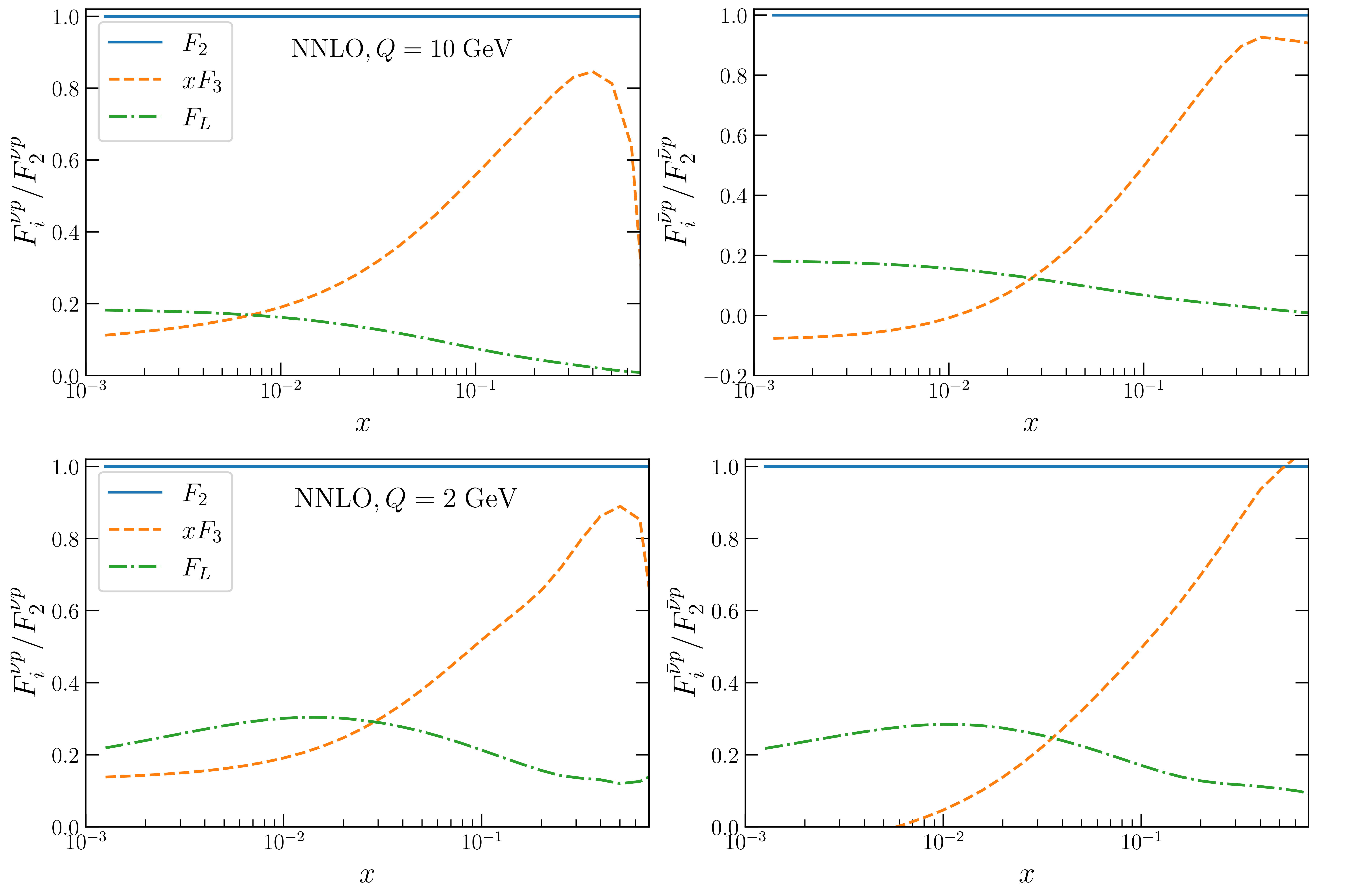

Stability of the Fits

Dataset	Target	Observable	$n_{\rm dat}$ (cuts)	$\chi^2_{\rm exp}$ (wo QCD)	$\chi^2_{\rm exp}$ (baseline)
BEBCWA59	Ne	F_2	57 (39)	1.673	2.088
		xF_3	57 (32)	0.842	0.771
CCFR	Fe	F_2	128 (82)	1.902	2.292
		xF_3	128 (82)	0.857	0.946
CDHSW	Fe	$[F_2]$	143 (92)	[6.17]	[5.32]
		$[xF_3]$	143 (100)	[22.9]	[11.7]
		$[F_W]$	130 (95)	[15.9]	[16.4]
		$d\sigma^{\nu}/dxdQ^2$	847 (676)	1.298	1.351
		$d\sigma^{\bar{\nu}}/dxdQ^2$	704 (583)	1.139	1.237
CHARM	$CaCO_3$	F_2	160 (83)	1.368	1.324
		xF_3	160 (61)	0.721	0.850
CHORUS	Pb	$[F_2]$	67 (53)	[63.8]	[38.3]
		$[xF_3]$	67 (53)	[6.881]	[2.904]
		$d\sigma^{\nu}/dxdQ^2$	606 (483)	0.986	1.185
		$d\sigma^{\bar{\nu}}/dxdQ^2$	606 (483)	0.709	0.797
NuTeV	Fe	$[F_2]$	78 (50)	[9.854]	[10.41]
		$[xF_3]$	75 (47)	[6.24]	[3.810]
		$d\sigma^{\nu}/dxdQ^2$	1530 (805)	1.436	1.542
		$d\sigma^{\bar{\nu}}/dxdQ^2$	1344 (775)	1.254	1.311
Total			**6197 (4089)**	**1.187**	**1.287**

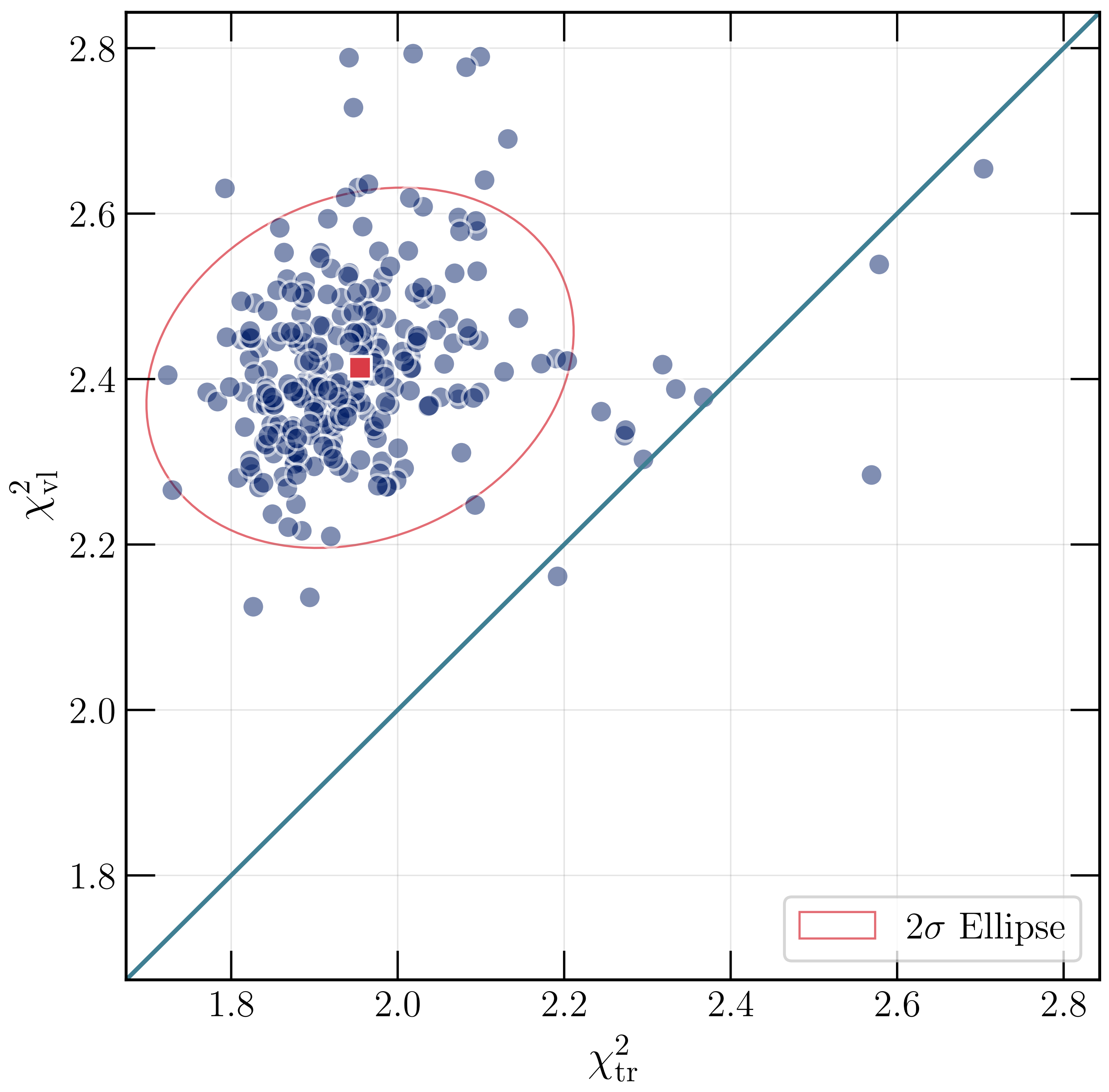

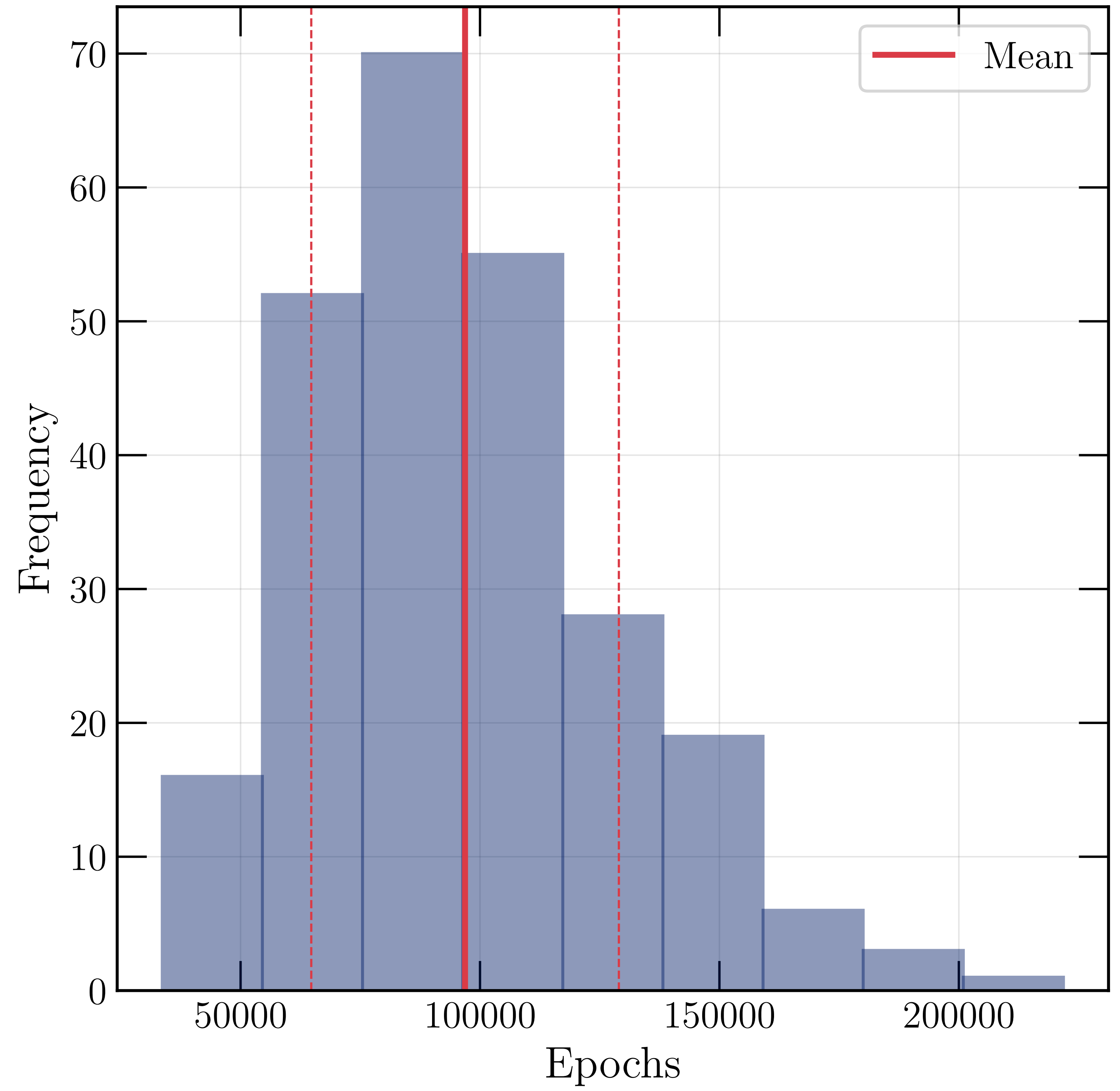

Experimental &is Theory Correlation Matrix

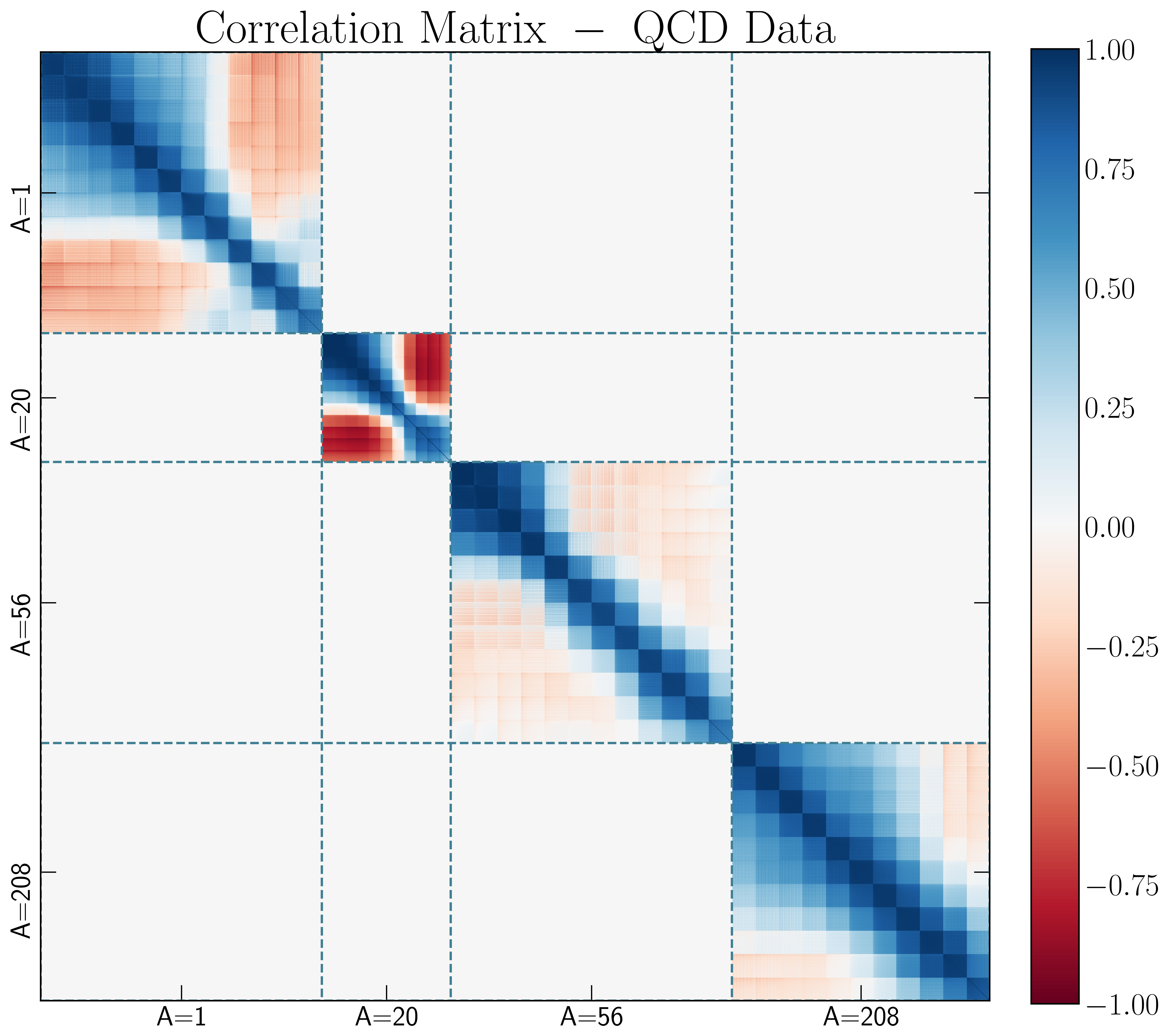

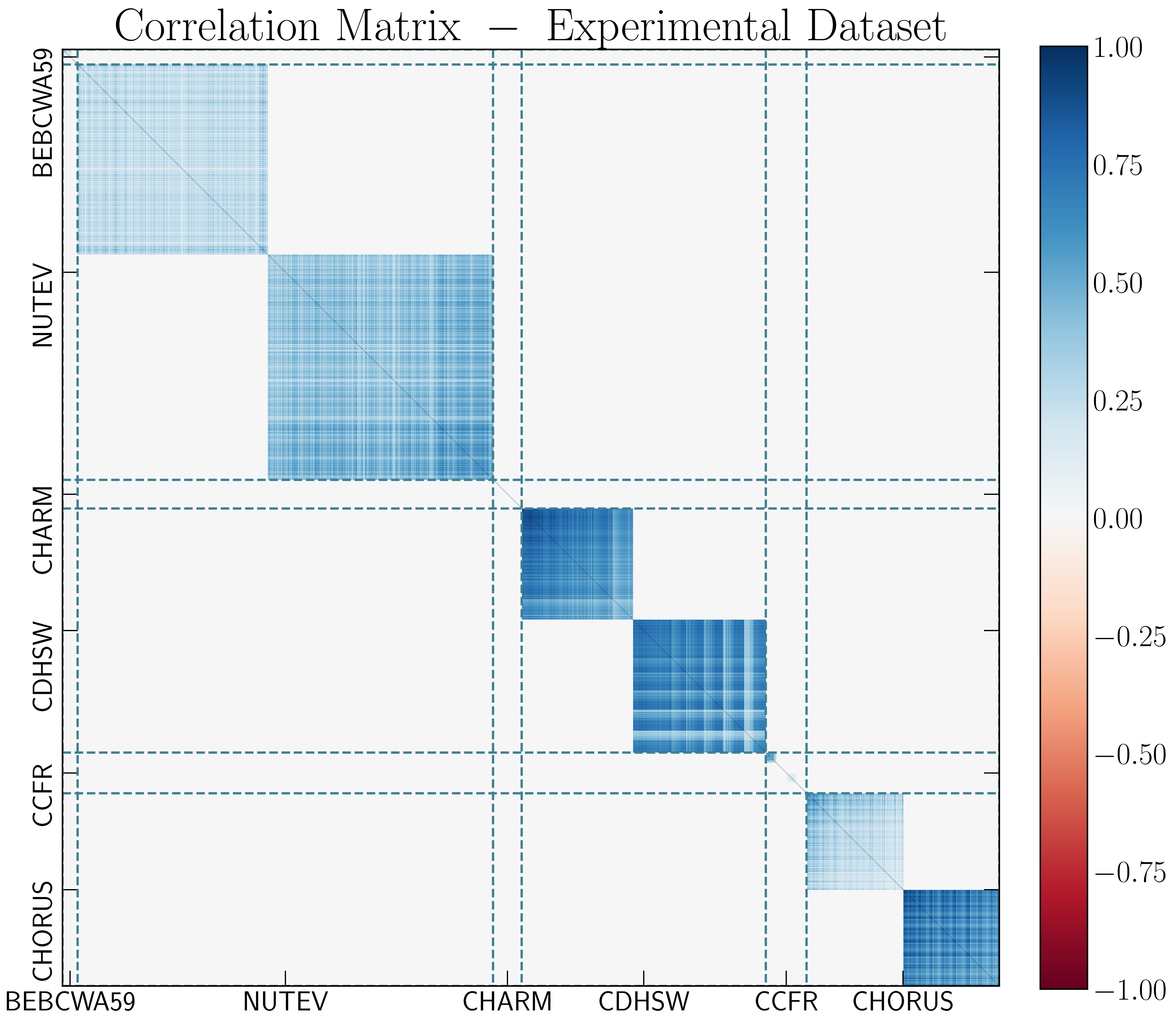

Matching Predictions along the Q^2 regions

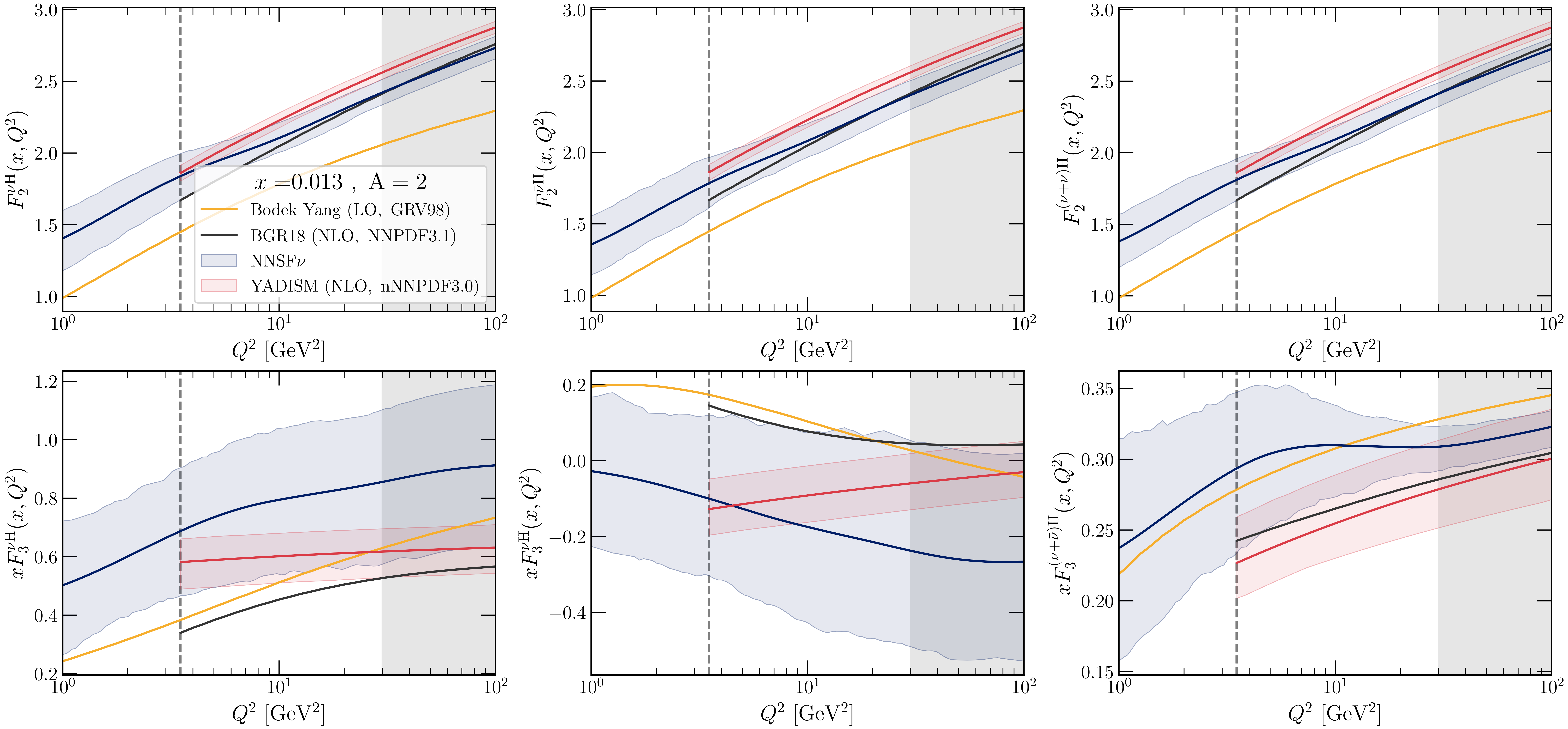

Predictions reproduce the pQCD constraints and are smooth along the entire region of Q^2

Dependence on the Q^2 cuts

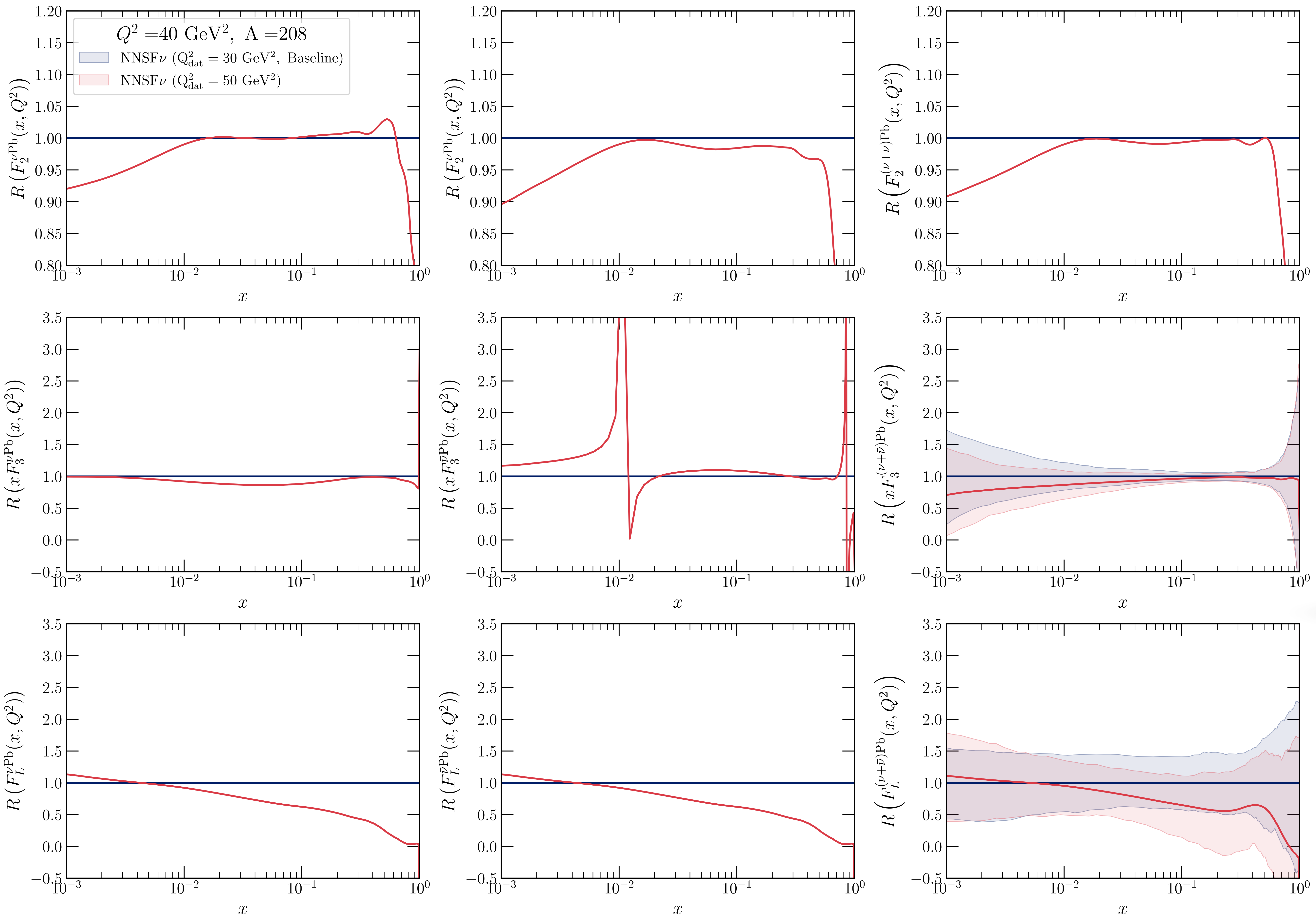

The choice of where to split the Q^2 regions yield **very small** differences. The largest differences occur in the extrapolation regions where no experimental data are available.

Predictions for the GLS sum rules

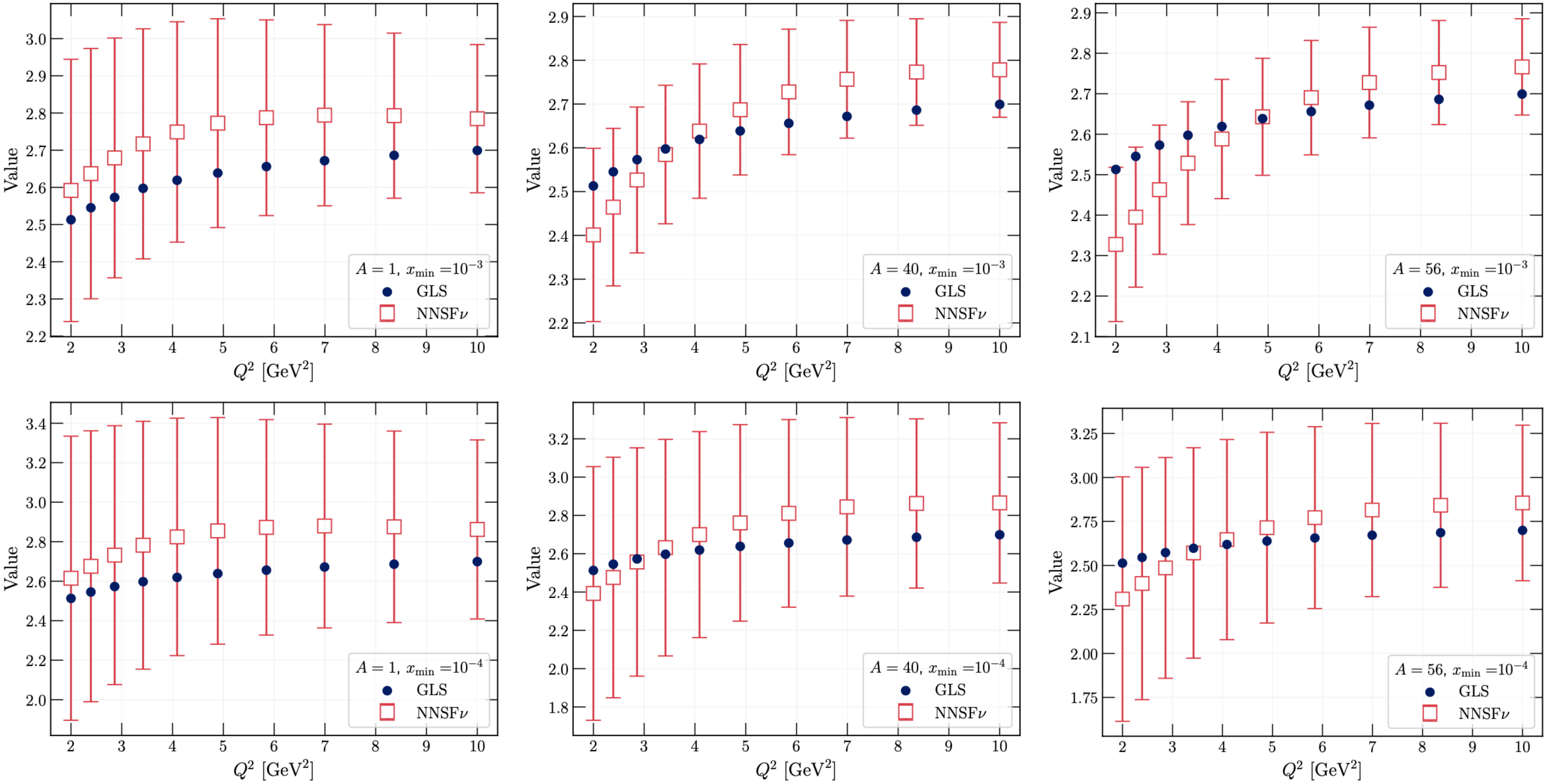

Inclusive Neutrino-Nucleus Cross-Sections